

## ABSTRACT

Title of Document: HETEROPHASE STEP-GROWTH  
POLYMERIZATION IN A CONTINUOUS  
TUBULAR REACTOR

Woo Jic Yang, Master of Science, 2013

Directed By: Professor Kyu Yong Choi  
Department of Chemical and Biomolecular  
Engineering

The interfacial process is a well-established industrial process for the production of Bisphenol A polycarbonates. However, there is a dearth of kinetic analyses of the interfacial process in a tubular reactor, which offers greater overall control of this process. In the interfacial process, Bisphenol A dissolved in a dispersed aqueous phase reacts with phosgene in the continuous organic phase producing oligomers that undergo further reaction in the organic phase to produce polymers. This process was carried out in a tubular reactor at a constant pressure of 85 PSI and a constant temperature of 35°C. The kinetics of the mass transfer and reaction and the solubility of reactants were used to develop a mathematical model of the interfacial process in a tubular reactor. The parameters were optimized using

proprietary plant data and the model simulations compared to the experimental data proved to be quite accurate. The developed model was used to investigate the heterophase kinetics of this system. A key parameter controlling the interfacial process in a tubular reactor is the dispersed aqueous droplet size. The droplet size determines the total surface area for mass transfer, and decreasing this droplet size from 10 $\mu$ m to 5 $\mu$ m results in an increase of molecular weight by about 130%. Also, the mass transfer coefficient of BPA ( $k_{L2}$ ) determines whether the processes at the interface are diffusion controlled or reaction controlled. The system exhibits diffusion controlled behavior when  $k_{L2}$  is approximately  $1.0 \times 10^{-7}$  m/s. Conversely, the system exhibits reaction controlled behavior when  $k_{L2}$  is around  $4.0 \times 10^{-6}$  m/s. The chain length distribution in the interfacial process follows Flory's most probable distribution. This functional group model was then expanded to a copolymerization system for siloxane-polycarbonate copolymers. For the copolymerization process, the key parameters shown to have a significant effect on the copolymer composition (mean sequence length and sequence length distribution) is the feed composition and reactivities of the comonomers.

HETEROPHASE STEP-GROWTH POLYMERIZATION IN A CONTINUOUS  
TUBULAR REACTOR

By

Woo Jic Yang

Thesis submitted to the Faculty of the Graduate School of the  
University of Maryland, College Park, in partial fulfillment  
of the requirements for the degree of  
Master of Science  
2013

Advisory Committee:  
Professor Kyu Yong Choi, Chair  
Assistant Professor Amy J. Karlsson  
Assistant Professor Dongxia Liu

© Copyright by  
Woo Jic Yang  
2013

## Acknowledgements

I would like to express my sincere gratitude to my advisor, Professor Kyu Yong Choi, for giving me this opportunity. His support, guidance, patience and encouragement made it possible to overcome many difficulties faced during my study.

I would like to thank the members of my dissertation committee, Professors Amy Karlsson and Dongxia Liu, for their valuable input and suggestions. I would also like to thank the faculty and staff of the Chemical and Biomolecular Engineering Department for their assistance.

I would like to acknowledge the financial support from LG Chem Ltd. Their support made it possible for me to attend graduate school without financial burdens. I would also like to express my appreciation for Bethany Presbyterian Church and the Bethany Scholarship Committee for their support throughout undergraduate and graduate studies.

I would like to thank all the members of our research group, In Hak Baick, Sangyool Lee, and Yunju Jung. They have helped me so much with their advice and suggestions. Thanks to the members of our research group, our lab was always a warm learning environment for me.

Special thanks go to my parents, Young Kook Yang and Kee Ok Yang, for their unconditional support and belief in me. I would not be here without them. I would also like to thank my sister, Eunmi Yang, for her positive outlook which always lifted my spirits, and my family in Korea, for their support.

All of this would not have been possible without the loving grace of God.

## Table of Contents

Chapter 1. Introduction.....	1
1.1 Background.....	1
1.2 Synthesis of Polycarbonates .....	4
1.2.1 Melt Transesterification Process.....	4
1.2.2 Interfacial Process.....	5
1.3 Literature Review.....	8
1.3.1 Analysis of Multiphase Interfacial Process in a Semibatch Reactor .....	8
1.3.2 Critical Process Parameters of the Interfacial Process in a Continuous Reactor .....	9
1.4 Objectives and Motivation.....	11
Chapter 2. Kinetics of the Interfacial Process in a Tubular Reactor .....	13
2.1 Tubular Reactor System.....	13
2.2 Interfacial Process Reaction Mechanism .....	15
2.3 Definition of Reaction Scheme.....	19
2.4 Dispersed Aqueous Phase Droplet Size.....	26
2.5 Derivation of Model Equations.....	30
2.6 Tubular Reactor Schematic.....	35
2.7 Parameter Estimation .....	36
2.8 Simulation Results .....	40
2.9 Polymer Chain Length Distribution.....	47
2.10 Effect of Bisphenol A Mass Transfer Rate on Polymer Properties .....	52
2.11 Conclusion .....	56
Chapter 3. Copolymerization.....	57
3.1 Introduction.....	57
3.2 Copolymerization Kinetics .....	60

3.3 Mean Sequence Length.....	65
3.3.1 Case I: Different Reactivities.....	69
3.3.2 Case II: Equal Reactivities.....	73
3.4 Sequence Length Distribution.....	76
3.4.1 Case I: Siloxane Injection in Point 1.....	77
3.4.2 Case II: Siloxane Injection in Point 2 .....	82
3.4.3 Case 3: Siloxane injection in Point 3 .....	86
3.5 Conclusion .....	89
Chapter 4. Summary .....	90

## Table of Figures

Figure 1.1 Reaction scheme for BPA-PC Melt Process .....	4
Figure 1.2 Reaction scheme for the Interfacial Process.....	6
Figure 2.1 SMX <sup>®</sup> static mixer is made up of a fixed structure inserted into a cylindrical pipe. A mixing element is also shown. ....	14
Figure 2.2 Stage 1 of the interfacial process: phosgenation. Interfacial reactions occur between di-sodium Bisphenate and phosgene or di-sodium Bisphenate and 2 phosgene. ....	15
Figure 2.3 Stage 2 of the interfacial process: polycondensation. Polymer forming reactions occur in the organic phase between 2 monochloroformates or a monochloroformate and a bischloroformate. ....	17
Figure 2.4 End capping reaction of the interfacial process.....	18
Figure 2.5 Definition of the chemical species for the functional group model. ....	19
Figure 2.6 The mass transfer and reaction process of the interfacial polymerization of PC in a tubular reactor. Mass transfer and reaction of BPA and phosgene at the interface lead to oligomer and polymers in the organic phase.....	21
Figure 2.7 The effect of flow rate on the droplet size distribution in a liquid-liquid dispersion in a 10mm diameter stainless steel tube packed with SMX <sup>®</sup> mixing elements. The fluids used were a water and Tween 80 mixture (aqueous phase) and cyclohexane (organic phase) [9]. ....	27
Figure 2.8 Relationship between linear velocity and average droplet size in a liquid-liquid dispersion. Data reported by Theron (flow rate vs. droplet size) was plotted to find a best fit curve for the linear velocity and droplet size relationship.....	28
Figure 2.9 Tubular Reactor System Schematic.....	35



Figure 2.10 Normalized concentration profiles for the BPA in the aqueous phase ( $A_o$ ), BPA at the interface ( $A_o^*$ ), phosgene in the organic phase ( $B_o$ ), and phosgene at the interface ( $B_o^*$ ). Simulation results.....	40
Figure 2.11 Normalized concentration profiles for para-tertiary butyl phenol ( $P_o$ ), modified para-tertiary butyl phenol ( $P_1$ ), and end-capped species ( $P$ ). Simulation results.....	41
Figure 2.12 Normalized concentration profiles for intermediate species: monochloroformate ( $A$ ), bischloroformate ( $B$ ); polymeric species: $Z_1$ , $Z_2$ ; and carbonate linkages ( $X$ ). Simulation results. .....	42
Figure 2.13 Evolution of normalized number average molecular weight ( $M_n$ ). Simulation results. .....	43
Figure 2.14 Comparison of experiment and predicted values of number average molecular weight and polymer production rate. ....	46
Figure 2.15 Flory's most probable distribution at three different positions along the tubular reactor (Zone B, Zone C, Zone D). Simulation results.....	49
Figure 2.16 The effect of dispersed aqueous droplet size on the specific surface area of interface and number average molecular weight obtainable. The relationship between drop size and molecular weight exhibits an exponential decay. Simulation Results.....	53
Figure 2.17 The effect of BPA mass transfer coefficient on the number average molecular weight obtainable. With small mass transfer coefficients, this process exhibits diffusion controlled behavior, while at large mass transfer coefficients, this process exhibits reaction controlled behavior. Simulation Results. ....	55
Figure 3.1 Siloxane inlets on tubular reactor system.....	63

Figure 3.2 Siloxane sequence length distribution (Siloxane inlet 1, $k_4=k_1/4$ , 10wt% Siloxane Feed)	77
Figure 3.3 Siloxane sequence length distribution (Siloxane inlet 1, $k_4=k_1/4$ , 20wt% Siloxane Feed)	78
Figure 3.4 Siloxane sequence length distribution (Siloxane inlet 1, $k_4=k_1/4$ , 30wt% Siloxane Feed)	79
Figure 3.5 Siloxane sequence length distribution (Siloxane inlet 1, $k_4=k_1/4$ , 40wt% Siloxane Feed)	80
Figure 3.6 Siloxane sequence length distribution (Siloxane inlet 2, $k_4=k_1/4$ , 10wt% Siloxane Feed)	82
Figure 3.7 Siloxane sequence length distribution (Siloxane inlet 2, $k_4=k_1/4$ , 20wt% Siloxane Feed)	83
Figure 3.8 Siloxane sequence length distribution (Siloxane inlet 2, $k_4=k_1/4$ , 30wt% Siloxane Feed)	84
Figure 3.9 Siloxane sequence length distribution (Siloxane inlet 3, $k_4=k_1/4$ , 10wt% Siloxane Feed)	86
Figure 3.10 Siloxane sequence length distribution (Siloxane inlet 3, $k_4=k_1/4$ , 20wt% Siloxane Feed)	87
Figure 3.11 Siloxane sequence length distribution (Siloxane inlet 3, $k_4=k_1/4$ , 10wt% Siloxane Feed)	88

## List of Tables

Table 2.1 The solubility of bischloroformate in an aqueous BPA solution.....	16
Table 2.2 Definition of kinetic rate constants.....	24
Table 2.3 Model Parameters Initial Estimates .....	36
Table 2.4 Proprietary Plant Data for Interfacial Process in Tubular Reactor (Normalized).....	38
Table 2.5 Optimized Parameter Values .....	38
Table 2.6 Experimental vs. Predicted Results for $M_n$ and Polymer Production Rate (Normalized) .....	45
Table 2.7 Normalized average molecular weight (Flory Distribution vs. Simulation results).....	50
Table 3.1 Examples of siloxane comonomers used for the synthesis of copolycarbonates [13]..	58
Table 3.2 Mean sequence length of Siloxane in copolymer (Inlet 1), $k_4=k_1/4$ .....	69
Table 3.3 Mean sequence length of Siloxane in copolymer (Inlet 2), $k_4=k_1/4$ .....	70
Table 3.4 Mean sequence length of Siloxane in copolymer (Inlet 3), $k_4=k_1/4$ .....	71
Table 3.5 Mean sequence length of Siloxane in copolymer (Inlets 1+2+3), $k_4=k_1/4$ .....	72
Table 3.6 Mean sequence length of Siloxane in copolymer (Inlet 1), $k_4=k_1$ .....	73
Table 3.7 Mean sequence length of Siloxane in copolymer (Inlet 2), $k_4=k_1$ .....	74
Table 3.8 Mean sequence length of Siloxane in copolymer (Inlet 3), $k_4=k_1$ .....	74
Table 3.9 Mean sequence length of Siloxane in copolymer (Inlets 1+2+3), $k_4=k_1$ .....	75

# **Chapter 1. Introduction**

## **1.1 Background**

Engineering thermoplastics are plastic materials that are used in applications requiring higher performance in areas such as heat resistance, chemical resistance, impact resistance, fire retardancy or mechanical strength. Engineering thermoplastics generally exhibit higher performance in one or more of these areas compared to commodity plastics. Polycarbonates (PC) have become a vital engineering thermoplastic in the plastic industry with excellent mechanical and optical properties as well as electrical and heat resistance that make it useful for many different engineering applications. They are commonly used as packaging materials, such as in water bottles and food containers, and are used in a wide range of applications including optics, mobile phones, electronic components, data storage, automotive and even medical applications [1].

The excellent properties of polycarbonates – particularly those derived from 2,2-bis(4-hydroxyphenyl)propane (bisphenol-A or BPA) – generated a large amount of research into this material in the late 1950s and ultimately resulted in the commercialization of BPA-derived polycarbonate processes by the late 1960s [2]. There are two major BPA-PC processes that have produced high quality resins and have remained economically viable. These two processes are

the two-phase interfacial (phosgene) and the melt transesterification (diphenyl carbonate or DPC) processes.

The bulk physical properties of a polymer, including polycarbonates, are determined by various structural properties of the polymer that can be controlled during the synthesis processes. For polycarbonate, the structural property that has the most influence on the physical properties is the chain length, or molecular weight. For example, with increasing chain length, polycarbonates exhibit an increase in melt and glass transition temperatures ( $T_g$ ), impact resistance, viscosity in the melt state, strength and toughness. The microstructure of polycarbonate also plays a role in determining the physical properties; linear, branched, and cross-linked polycarbonates of the same average molecular weight may exhibit different physical properties. In linear polycarbonates, the flow properties depend only on the molecular weight. However, branched polycarbonate exhibits improved flow properties which depend on the molecular weight and degree of branching [3]. Further, linear polycarbonates suffer from low surface hardness and relatively poor solvent resistance. These properties can be significantly improved by cross-linking BPA-PC [4].

Another approach to improving the physical properties of polycarbonates is the addition of copolymers to polycarbonate which can improve weatherability (UV stability), thermal stability and fire retardancy. One prime example of this is copolymers of BPA-PC and polydimethylsiloxane (PDMS) which have been investigated since the early 1960s [2]. Recently, siloxane-polycarbonate block copolymers have been the subject of much interest. The siloxane block in these copolymers lead to low  $T_g$ , excellent thermal stability and good weathering properties. Siloxane-polycarbonate copolymers can be produced by introducing functionalized

siloxane blocks in the interfacial polymerization process with BPA and phosgene, or in the melt process with high molecular weight PC.

## 1.2 Synthesis of Polycarbonates

### 1.2.1 Melt Transesterification Process

The melt process involves the step-growth condensation reaction between equimolar amounts of BPA and DPC in the presence of a catalyst such as lithium hydroxide and produces phenol as a by-product. The reaction scheme for this process is shown in Figure 1.1 below.

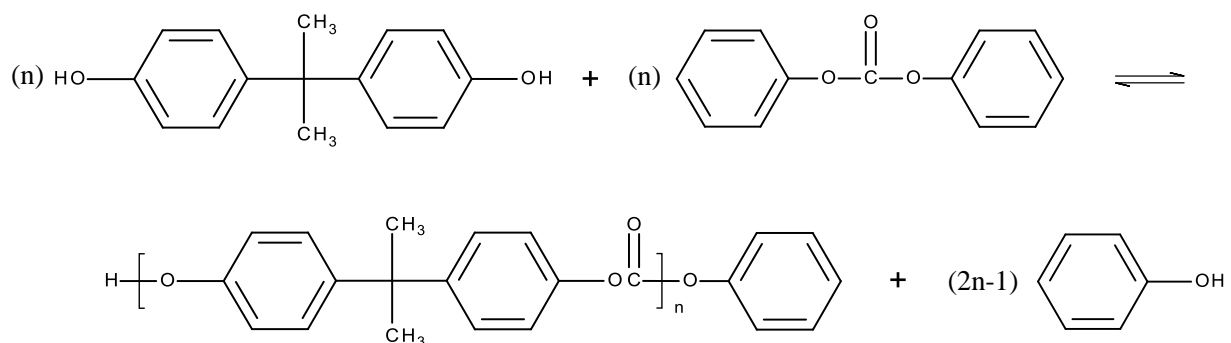


**Figure 1.1** Reaction scheme for BPA-PC Melt Process

This reaction is run at sufficiently high temperatures to keep the reactants and products molten (150-350°C). The transesterification is an equilibrium reaction, thus the effective removal of phenol, the by-product, is crucial to driving the reaction and producing high quality, high molecular weight. The removal of phenol is also important because side reactions involving phenol produces discoloration of polycarbonate. Phenol can be removed from the reaction

mixture at high temperature and low pressure. Thus, the reaction pressure is reduced from 760 mmHg to less than 1 mmHg [2].

The melt process is advantageous because the process scheme is relatively simpler than the interfacial polymerization process, the polymer can be obtained in undiluted form which can be directly pelletized and does not involve toxic chemicals such as phosgene gas and methylene chloride [5]. However, this process has some disadvantages. In addition to the problem of removing phenol from the reaction mixture, some discoloration occurs due to high reaction temperatures, and there are difficulties in obtaining high molecular weight PC and in the removal of phenol due to the high melt viscosity of PC.

### 1.2.2 Interfacial Process

In the interfacial process, phosgene is used instead of DPC. Phosgene gas is added to a two phase mixture of an aqueous alkaline solution of the sodium salt of BPA (di-sodium Bisphenate) and a water-immiscible solvent such as methylene chloride (organic phase) and the reaction mixture is maintained as an emulsion by vigorous agitation, where the former is the dispersed phase and the latter is the continuous phase. The phosgene gas that is added to this reaction mixture is dissolved in the organic phase, where it can react with di-sodium Bisphenate at the interface of the aqueous and organic phases. The reaction scheme of this process is summarized in the Figure 1.2.



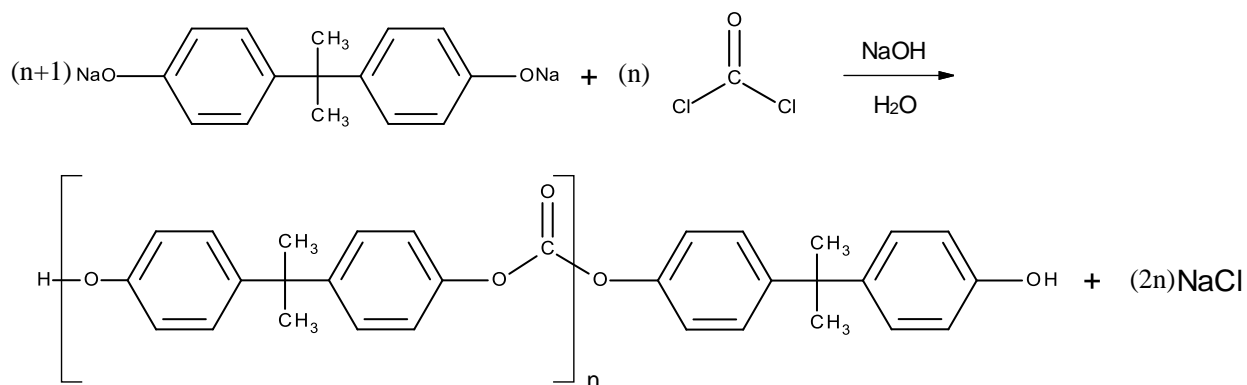


**Figure 1.2** Reaction scheme for the Interfacial Process

The interfacial process is comprised of two steps: the phosgenation of BPA at the interface, followed by polycondensation in the organic phase to produce polycarbonate. An end-capping agent, usually a monohydroxylic phenol such as para-tertiary butyl phenol (PTBP), is added to the reaction mixture to inactivate some of the reactive end groups produced in this process to control the molecular weight of the polymer and to stabilize the polymer for downstream processing. Throughout the process, the pH of the reaction mixture is maintained between 9 and 12. The reaction scheme of this process will be discussed in more detail in Chapter 2.

Among the advantages of this process are the relatively low reaction temperature (40°C) and the ability to produce polymers of very high molecular weight (up to 200,000 Da) in relatively short reaction times [1]. However, this process presents several disadvantages from a

technological and environmental point of view. First, this process involves the use of toxic chemicals such as phosgene and methylene chloride which can pose some environmental problems. Further, because the polymer is produced in a heterogeneous mixture, the methylene chloride from the polymer solution must be removed but the complete removal is difficult and requires a significant amount of energy since methylene chloride has a strong affinity to polycarbonate. Residual chlorine impurities may have negative effects on the end user properties of the polymer obtained. Finally, the final product must undergo several washing step: with a dilute acid to neutralize the caustic material, with water to remove the by-product, NaCl, and with a dilute caustic solution to eliminate any unreacted BPA.

## 1.3 Literature Review

### 1.3.1 Analysis of Multiphase Interfacial Process in a Semibatch Reactor

Perhaps the only publication on the theoretical analysis of an interfacial polymerization of polycarbonate in an isothermal semi-batch reactor is by Patrick Mills [6]. In his study, a well-mixed, liquid-liquid dispersion system was considered with the dispersed aqueous phase initially containing BPA and NaOH and the continuous phase containing phosgene and methylene chloride. Additionally, in this reactor system, phosgene gas was added as bubbles to initiate the reaction and the volumetric flow rate of phosgene was kept constant. Mass transfer resistances between the various phases were described using the two-film theory but only the mass transfer of small molecules such as phosgene, BPA and a mono-functional chain stopper was considered. Due to the unavailability of fundamental kinetic data, the significance of the reactions that occur at the liquid interface compared to the reactions that occur in the bulk phase could not be determined. Thus, only estimates of reactor performance based on the two-film theory with reaction that occurring in the bulk phase was considered. The equal reactivity of end-groups was considered for simplicity, and all reactions were assumed to exhibit elementary behaviors in terms of reaction order.

Using the assumptions listed above, an infinite set of differential equations was derived whose solutions results in the concentration of each species as a function of time, chain length, and other chemical parameters. Although equations were derived considering the mass transfer and reaction of the small molecules discussed previously, to further simplify these equations it was assumed that the liquid-liquid mass transfer rate was much more rapid than the rate of the reactions, thus eliminating all liquid-liquid mass transfer terms (i.e., reaction control process).

The mass transfer of phosgene from the gas phase to the organic phase was considered. However, an assumption was made that the mass transfer of phosgene to the aqueous phase occurs through the organic phase, as the gas bubbles are not in contact with the dispersed aqueous phase. The  $z$ -transform method was used to reduce this set of equations to a finite set of ordinary differential equations. The solution to these reduced equations yielded the concentration of each species as the first three moments of the polymer chain length distribution. The moments were used to determine the instantaneous number and weight average molecular weight of the polymer.

Mills used his model to investigate the parametric sensitivity of the system by varying the initiation and propagation rate constants for both negligible and finite gas-liquid mass transfer resistances. The values for the initiation rate constant varied from 0.0001 to 0.005 and the values for the propagation rate constant varied from 0.0001 to 0.01. He calculated the conversion of monomers, concentration profiles of the various polymer species, the number and weight average molecular weight profile and chain length distribution. From the technical report by Mills, we can gain some insights into the assumptions needed to investigate the interfacial reactions and we can also obtain the estimates of the kinetic rate constants.

### 1.3.2 Critical Process Parameters of the Interfacial Process in a Continuous Reactor

In another study by Gu and Wang [7] on interfacial polycarbonate reactions, the critical process parameters of the continuous interfacial process is investigated. In this study, experimental work was conducted in an effort to understand the process parameters of this process. Since the batch phosgenation process is complicated by simultaneous oligomerization and because only a few qualitative descriptions of the intermediates have been reported in

literature, a semi-continuous process was developed in which the phosgenation and oligomerization is controlled separately. In this system, an organic solution comprised of phosgene dissolved in methylene chloride and a caustic, aqueous solution of BPA is fed to a series of static mixers that act as a plug flow reactor for the continuous phosgenation. The effluent from the static mixers is fed to a batch reactor where the oligomerization and polycondensation reactions occur. The effluent from the static mixers was analyzed using high-performance liquid chromatography (HPLC).

The following conclusions were made about the continuous phosgenation process in this study.

1. The ratio of bischloroformates to monochloroformates increases with higher phosgene to BPA ratios.
2. The conversion of BPA increases with increasing organic phase to aqueous phase volume ratio.
3. Conversion of BPA increases with increasing linear velocity which promotes better mixing of the two phases until the decrease in residence time starts to decrease the conversion.
4. In order to have complete phosgenation of BPA, the excess phosgene must be 5-8 mol% of BPA.
5. Monochloroformate was found to have a much higher reactivity than bischloroformate.

These conclusions drawn from the analysis of a continuous phosgenation process provides much insight into the assumptions needed to model the interfacial process.

## 1.4 Objectives and Motivation

Despite the considerable amount of study that has been done concerning the chemistry and physics of bisphenol-A polycarbonate since the 1950s, chemical engineering analyses of the polymerization kinetics have not been reported until much more recently. Furthermore, although the interfacial process for BPA-PC synthesis is a well-established industrial technology, little has been reported on the mathematical modeling of this process. Also, there is a dearth of open literature on the scientific and engineering aspects of industrial polymerization processes, particularly on the relevant reaction kinetics. Due to the impossibility of conducting experimental work in an academic research environment, it is desired that any development of novel polycarbonate products, such as co-polycarbonates, should be developed based on a quantitative reaction process model. It is our aim to investigate the fundamental reaction kinetics of the interfacial process and develop a mathematical model of the interfacial polymerization of PC in a tubular reactor.

In Mills [6], the developed process model only considered the reactions that occur in the bulk phase. However, the reaction that occurs at the interface proved to be vital to this process, as it is the initiation of the interfacial process. Thus, we aim to consider the mass transfer and reaction that occurs at the interface between di-sodium Bisphenate and phosgene. We also investigate the effects of various reactor parameters, such as dispersed aqueous droplet size that have a direct impact on the rate of mass transfer of phosgene and di-sodium Bisphenate to the interface.

Due to the added complexity of considering the mass transfer and reaction at the interface and the computational burden of a population balance using a molecular species model, we

implement a simpler functional group model that can still predict important properties of interfacial PC, such as number average molecular weight, molecular weight distribution (both of which have a significant impact on the physical properties of the polymer), and total polymer yield.

Modeling of the interfacial process in a semi-batch reactor has been reported by Mills, but currently, there are no publications regarding the modeling of the interfacial polymerization of PC in a tubular reactor (PFR). Our aim was to investigate the fundamental reaction kinetics of the interfacial process, to develop a comprehensive, functional group model that can accurately predict this process in a tubular reactor and to extend this model to a copolymerization process.

## **Chapter 2. Kinetics of the Interfacial Process in a Tubular Reactor**

### **2.1 Tubular Reactor System**

As discussed in Section 1.3, computational kinetic rate analyses of the interfacial process have been published [6,7]. These works are related to the production of polymer in both batch and semibatch processes. Our study involves the mathematical modeling of the kinetics of the interfacial process in a continuous plug flow reactor. There are many advantages of using a PFR rather than a batch or semibatch reactor. From an industrial standpoint, PFRs exhibit higher conversion per unit volume, have lower operating costs, and can be operated continuously. Further, PFRs offer greater overall control of the process. This can be attributed to the fact that in a PFR, the distribution of residence time is much narrower than in a stirred tank reactor, that is, in a PFR, all reactants experience the same residence time. For a condensation reaction, as it is in the case of the interfacial process, the molecular weight distribution (MWD) is strongly affected by the residence time distribution (RTD) [8].

In a stirred tank reactor, the dispersion of the two immiscible phases is maintained via mechanical agitation. In a PFR, such methods cannot be utilized. Instead, an in-line, static mixer can be used to establish a plug flow profile in the reactor. Many different types of in-line static mixers are commercially available. Static mixers are motionless mixers consisting of fixed structures inserted into cylindrical pipes. Liquid-liquid dispersions are achieved by passing the



two immiscible liquid cocurrently through the mixers. A SMX<sup>®</sup> static mixer is shown in Figure 2.1. In a recent study on turbulent liquid-liquid dispersion in SMX<sup>®</sup> mixers [9], it has been shown that SMX<sup>®</sup> mixers exhibit more efficient mixing than mechanical agitation in a stirred tank reactor. This is because SMX<sup>®</sup> mixers dissipate energy more uniformly with all droplets being exposed to fairly uniform shear stress as they pass through the media. Thus, not only do SMX<sup>®</sup> mixers offer a lower operating cost, they provide better control of dispersed droplet size and droplet size distribution. The main parameters that control the droplet size are length of mixer, number of mixers, and flow rate through the mixers. In our reactor system, the tubular reactor is assumed to be equipped with such internal mixing elements to warrant a perfect mix in the radial direction.

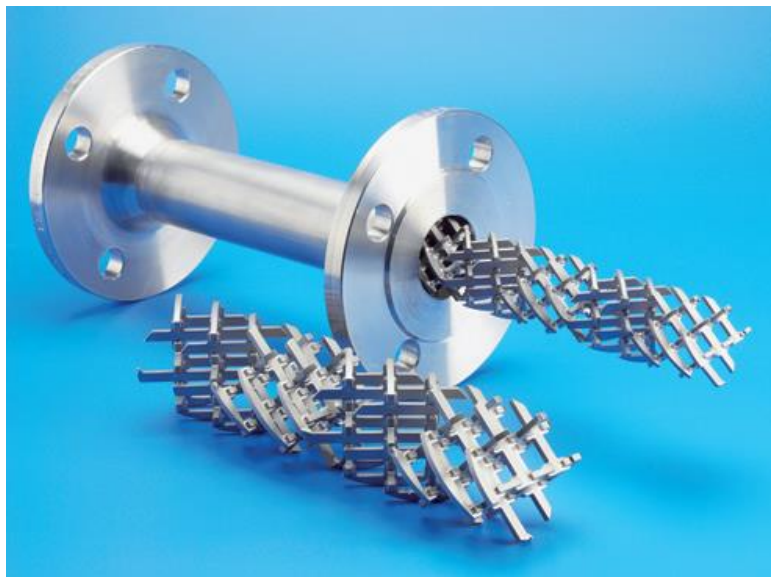


**Figure 2.1** SMX<sup>®</sup> static mixer is made up of a fixed structure inserted into a cylindrical pipe. A mixing element is also shown.

## 2.2 Interfacial Process Reaction Mechanism

As discussed briefly in Section 1.2.2, the interfacial process involves the reaction between BPA dissolved in a dispersed, caustic, aqueous phase, and phosgene dissolved in the continuous, organic phase (methylene chloride). The polymerization occurs in two distinct stages as shown in the following two figures [2].

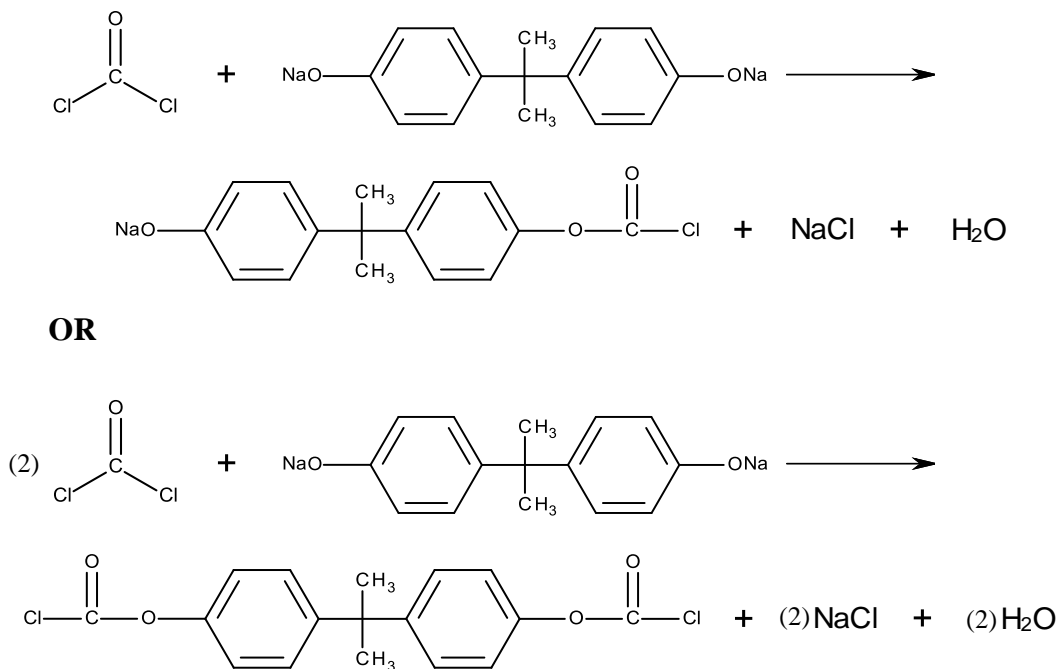


**Figure 2.2** Stage 1 of the interfacial process: phosgenation. Interfacial reactions occur between di-sodium Bisphenate and phosgene or di-sodium Bisphenate and 2 phosgene.

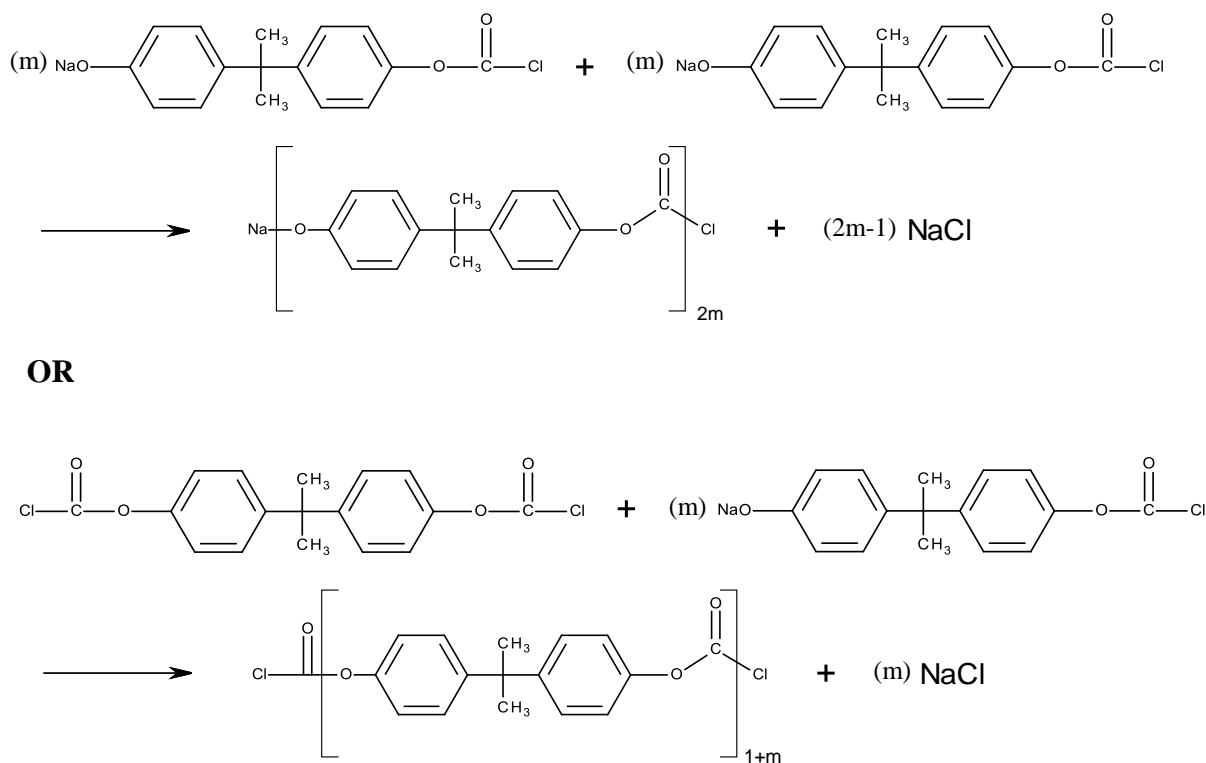
The first stage, phosgenation, as seen in Figure 2.2, is the reaction between di-sodium Bisphenate (in the aqueous phase) and phosgene (in the organic phase) at the interface between the dispersed aqueous phase and the continuous organic phase. BPA is practically insoluble in methylene chloride [10] as phosgene is insoluble (actually only slightly soluble) in the aqueous phase [11]. Thus, the two monomers are assumed to react only at the interface of the organic and aqueous phases. Di-sodium Bisphenate can react with one phosgene molecule to yield bisphenol-A monochloroformate. Another possible reaction in this first stage is the reaction between two phosgene molecules and di-sodium Bisphenate, bisphenol-A bischloroformate is produced.

**Table 2.1** The solubility of bischloroformate in an aqueous BPA solution

	<b>Solution 1</b>	<b>Solution 2</b>	<b>Solution 3</b>	<b>Solution 4</b>	<b>Solution 5</b>
<b>NaOH Concentration</b>	1.29 mol/L	1.29 mol/L	1.29 mol/L	1.29 mol/L	1.29 mol/L
<b>BPA Concentration</b>	0.63 mol/L	0.5 mol/L	0.38 mol/L	0.25 mol/L	0 mol/L
<b>Bischloroformate Solubility</b>	< 60 ppm	< 60 ppm	< 60 ppm	< 60 ppm	< 60 ppm

To further understand the dynamics of this two phase system, a series of solubility experiments were carried out to determine the solubility of short oligomers in the aqueous phase, as we know that the polymer is not soluble. The aqueous phase in this process is made up of three components: water, BPA, and sodium hydroxide. Thus, we prepared a series of solutions (listed in Table 2.1) with decreasing content of BPA to simulate the consumption of BPA during the reaction process. The short chain oligomer that was tested is bisphenol-A bischloroformate (bischloroformate) purchase from Sigma-Aldrich. After the solutions were prepared, the

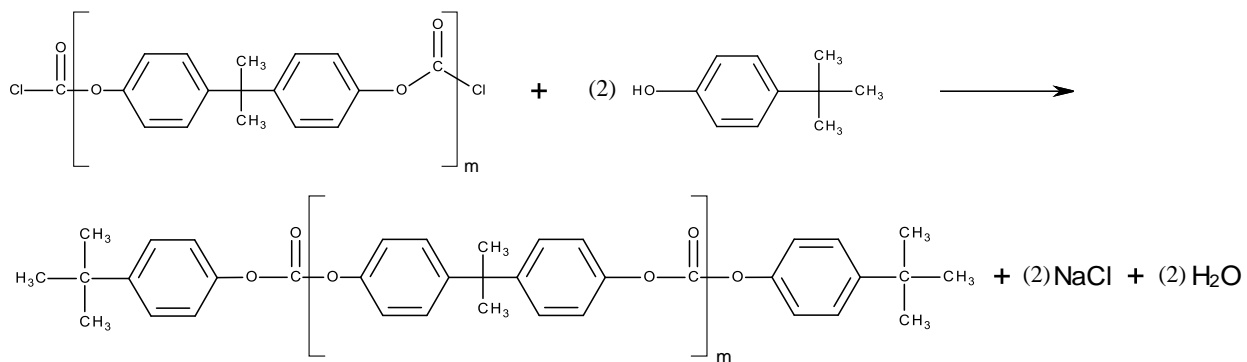
solubility of bischloroformate was tested by adding 20 mg/ml to 50 milliliters of each of the 5 different aqueous solutions. Showing no signs of solubility in this solvent, the amount of bischloroformate added to the aqueous solutions was decreased down to 0.06 mg/ml (60 ppm). The results showed that bischloroformate was not soluble in any of the aqueous solutions. Thus we assume that the solubility of chloroformates in the aqueous phase is insignificant and can be ignored in this model. Due to favorable solubility in the organic phase, mono/bischloroformates are assumed to be transferred to the organic phase instantaneously where the next step in the interfacial process occurs.



**Figure 2.3** Stage 2 of the interfacial process: polycondensation. Polymer forming reactions occur in the organic phase between 2 monochloroformates or a monochloroformate and a bischloroformate.

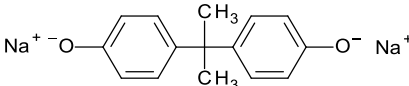
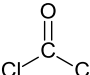
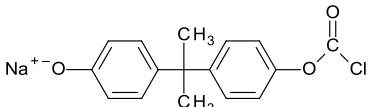
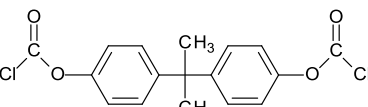
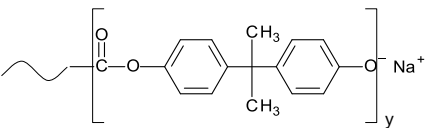
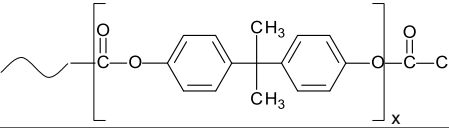
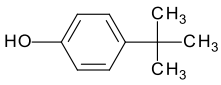
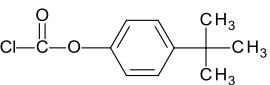
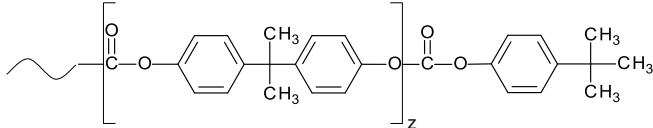
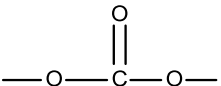
Figure 2.3 depicts the second stage of the interfacial process, polycondensation. Polycondensation, the formation of oligomers and polymers, occurs solely in the organic phase. In this stage, two reactions occur: the reaction between two monochloroformates or the reaction between a monochloroformate and a bischloroformate. These reactions produce PC oligomers that differ in functional end groups. These oligomers further react with chloroformates or other oligomers, depending on available functional groups, to produce long chain polymers.

The final step in the interfacial process is the addition of an end capping agent, or chain stopper, to control the molecular weight of the polymer and to stabilize the remaining reactive end groups. This reaction is illustrated in Figure 2.4.



**Figure 2.4** End capping reaction of the interfacial process

### 2.3 Definition of Reaction Scheme.

<u>Chemical Species</u>	<u>Label</u>
	$A_0$
	$B_0$
	$A$
	$B$
	$Z_1$
	$Z_2$
	$P_0$
	$P_1$
	$P$
	$X$

**Figure 2.5** Definition of the chemical species for the functional group model.

To summarize the reaction process, phosgene ( $B_o$ ) and di-sodium Bisphenate ( $A_o$ ) migrate from their respective bulk phases (organic phase for phosgene and aqueous phase for di-sodium Bisphenate) to the interface to react. Di-sodium Bisphenate and phosgene at the interface are denoted by  $A_o^*$  and  $B_o^*$ , respectively. The transfer of these two reactants to the interface is described using the two film theory. Upon reaction of these two species at the interface, monochloroformate BPA (A) is generated. Species A in the organic phase can then react with phosgene in the bulk, organic phase to generate bischloroformate BPA (B). Since bischloroformate BPA is not soluble in the aqueous phase, the reasonable assumption would be that monochloroformate BPA is not soluble in the aqueous phase also. Thus, monochloroformate BPA, which is generated from the reaction at the interface, precipitates out into the organic phase. Species A and B act as the monomer units that react in the organic phase to generate oligomers and, eventually, polymer species. Since species A and B are constantly being generated as the reaction proceeds, both species are available to react with the growing polymer chains (species  $Z_1$  and  $Z_2$ ).  $Z_1$  and  $Z_2$  represent the growing polymer chains, each differentiated by a distinct functional group. Further, species  $Z_1$  and  $Z_2$  only react with monomer units A and B, but also with each other. The chain stopper para-tertiary butyl phenol ( $P_o$ ) is present in the organic phase. PTBP can react with phosgene in the organic phase which changes its functional end group ( $P_1$ ). The chain stopper can react with the monomer units (A and B) and with the growing polymer chains producing end-capped species (P). This reaction process is depicted in Figure 2.6.

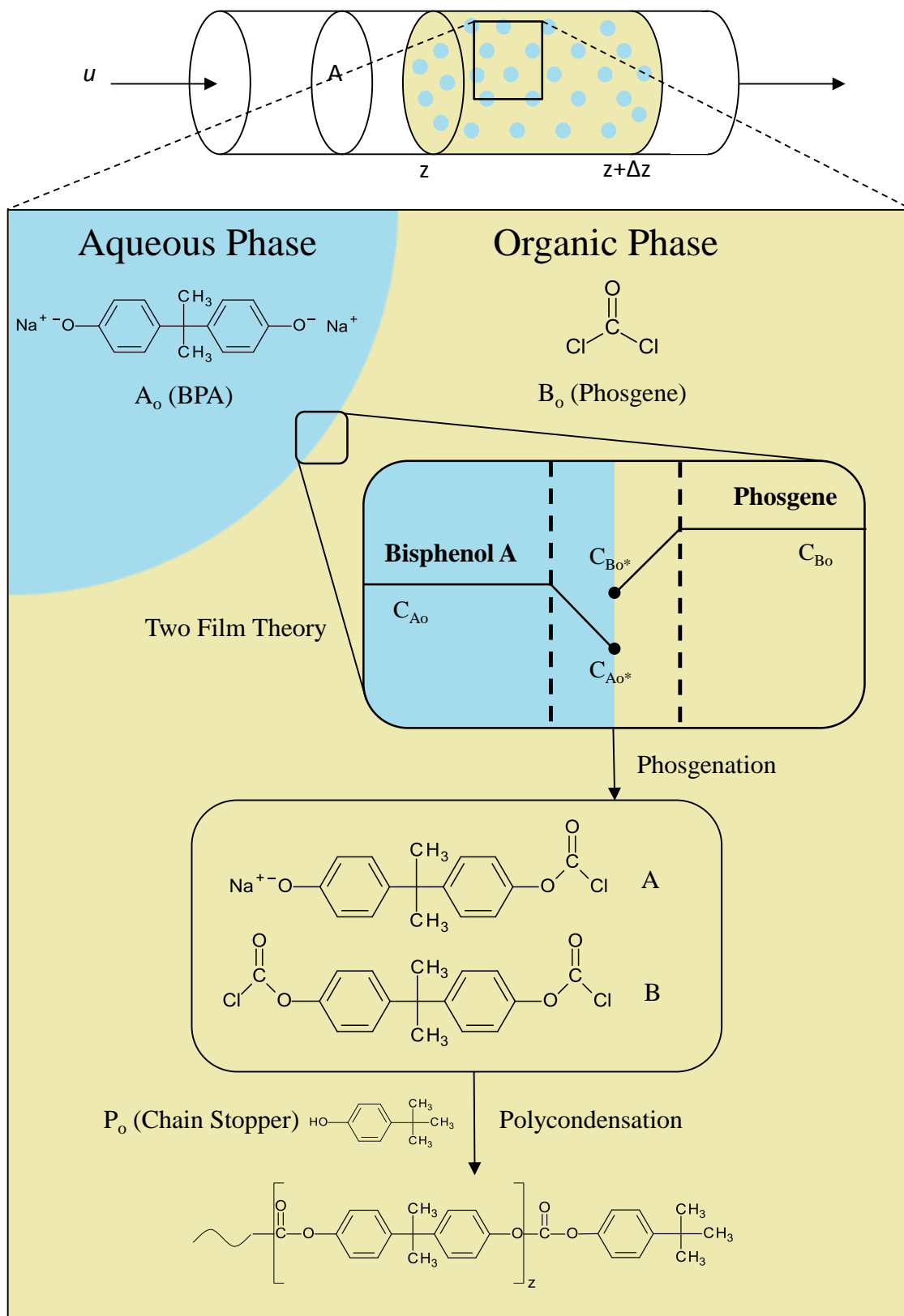


**Figure 2.6** The mass transfer and reaction process of the interfacial polymerization of PC in a tubular reactor. Mass transfer and reaction of BPA and phosgene at the interface lead to oligomer and polymers in the organic phase.

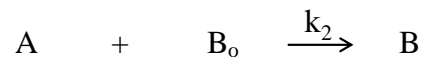


Based on the assumptions proposed above, the following scheme has been derived:

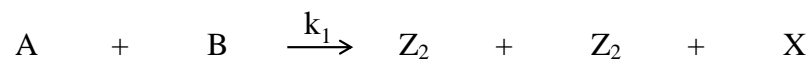
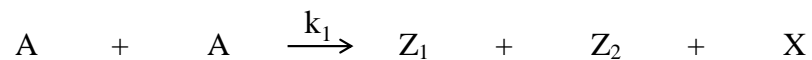
- **Phosgenation** (interface)



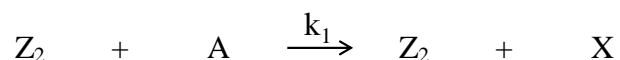
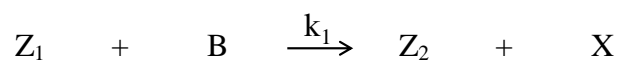
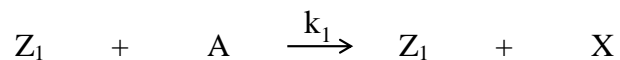
- **End unit conversion of monomer units** (organic phase)



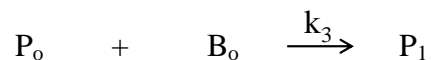
- **Reactions between monomer units** (organic phase)



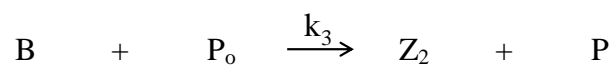
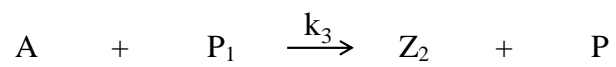
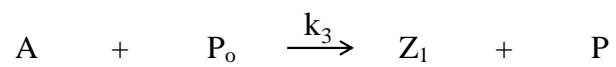
- **Reactions between monomer units and polymer species** (organic phase)



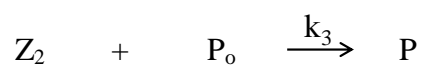
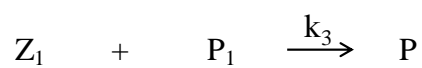
- **Chain stopper end unit conversion** (organic phase)



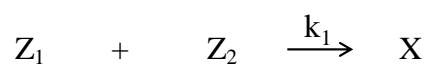
- **Reactions between monomer units and chain stopper** (organic phase)



- **Reactions between polymer species and chain stopper** (organic phase)



- **Reactions between polymer species** (organic phase)



For this set of chemical reactions, we define the following kinetic rate constants.

**Table 2.2** Definition of kinetic rate constants

<b>Rate Constants</b>	<b>Definition</b>
$k_1$	Kinetic rate constant for polymerization, including the phosgenation reaction at the interface, in units of $\text{m}^3/\text{mol sec}$
$k_2$	Kinetic rate constant for phosgene reaction in the bulk (organic) phase, in units of $\text{m}^3/\text{mol sec}$
$k_3$	Kinetic rate constant for PTBP in the bulk phase, in units of $\text{m}^3/\text{mol sec}$
$k_{L1}$	Mass transfer coefficient of phosgene, in units of $\text{m}/\text{sec}$
$k_{L2}$	Mass transfer coefficient of BPA, in units of $\text{m}/\text{sec}$

In the reaction scheme above, species X represents the carbonate linkages between monomer units in the polymer species. The number of carbonate linkages generated during the interfacial polymerization process is tracked so that the calculation of the number average molecular weight is possible in our simulation model.

The reactions at the interface and the end unit conversion of monomer units do not generate any carbonate linkages. For the reactions between monomer units, each reaction generates one carbonate linkage. Further, each reaction generates a growing polymer chain with

two functional end groups on each end. Reactions between A and A produces one  $Z_1$  (a sodium Bisphenate end group) and one  $Z_2$  (a chloroformate end group). Reactions between A and B produces two  $Z_2$  end groups on both chain ends. For the reactions between monomer units and growing polymer species, one functional end group of a growing polymer chain reacts with a monomer unit, each reaction generating one carbonate linkage. The functional end group is consumed as it reacts with a monomer species but a new functional end group is generated depending on which monomer unit reacted. The chain stopper end unit conversion reactions do not produce any carbonate linkages. The reactions between monomer units and chain stoppers do not produce any carbonate linkages as well. The chain stopper reacts with one functional end group of a monomer unit leaving the other functional end group available to participate in further reactions occurring in the organic phase. For the reactions between polymer species and chain stoppers, the chain stopper reacts with the functional end group of a growing polymer chain which results in a capped end group that no longer can react. Again, in these reactions, no carbonate linkages are produced. Lastly, in the reactions between polymer species, the reactive end groups of each growing polymer chain react with each other to consume both reactive end groups, creating one carbonate linkage.

## 2.4 Dispersed Aqueous Phase Droplet Size

One of the major issues to be addressed in modeling the phosgenation process is that the mass transfer and reaction of BPA and phosgene at the interface of suspended liquid droplets should be quantitatively described. The rate of interfacial mass transfer is dependent on the interfacial reactant concentrations and the available droplet surface area or specific surface area,  $a$  ( $\text{cm}^2/\text{cm}^3$ ), which is dependent upon the size of aqueous droplets. In our reactor system, the aqueous phase is forced to flow through a tubular section packed with SMX<sup>®</sup> static mixers where the aqueous phase is ‘ground’ to small droplets suspended in a continuous organic phase (methylene chloride). The rate of mass transfer is hence dependent on the total available surface area, which is a function of bubble size and bubble holdup. Therefore, it is necessary to investigate the effects of aqueous droplet size on the performance of phosgenation reaction. It is reasonable to expect that the static mixers provide intensive mixing and turbulence to generate as large a surface area so to eliminate mass-transfer limitation in this heterogeneous process. Nevertheless, we need to incorporate the mass transfer effects in the reactor model. In short, we need to estimate the average droplet size and available specific surface area.

According to Theron [9], in a SMX<sup>®</sup> mixer with fixed length and fixed number of mixing elements, the size of dispersed droplets in a liquid-liquid dispersion depends on the flow rate through the mixer. At a given flow rate, the mean energy dissipation rate per mass unit can be regarded as a measure of turbulence at any point in the mixer, thus, the addition of mixers does not alter the intensity of the turbulence. High flow rates produce a finer dispersion at equilibrium and require shorter residence times to reach equilibrium. Figure 2.7, illustrates the effect of liquid flow rate on the droplet size distribution for several different flow rates. The data show that larger droplets (smaller specific surface area) are obtained as the flow rate is smaller.

Also, this figure illustrates that the droplet sizes are fairly broadly distributed, but in this model, the average droplet size will be adopted for simplicity.

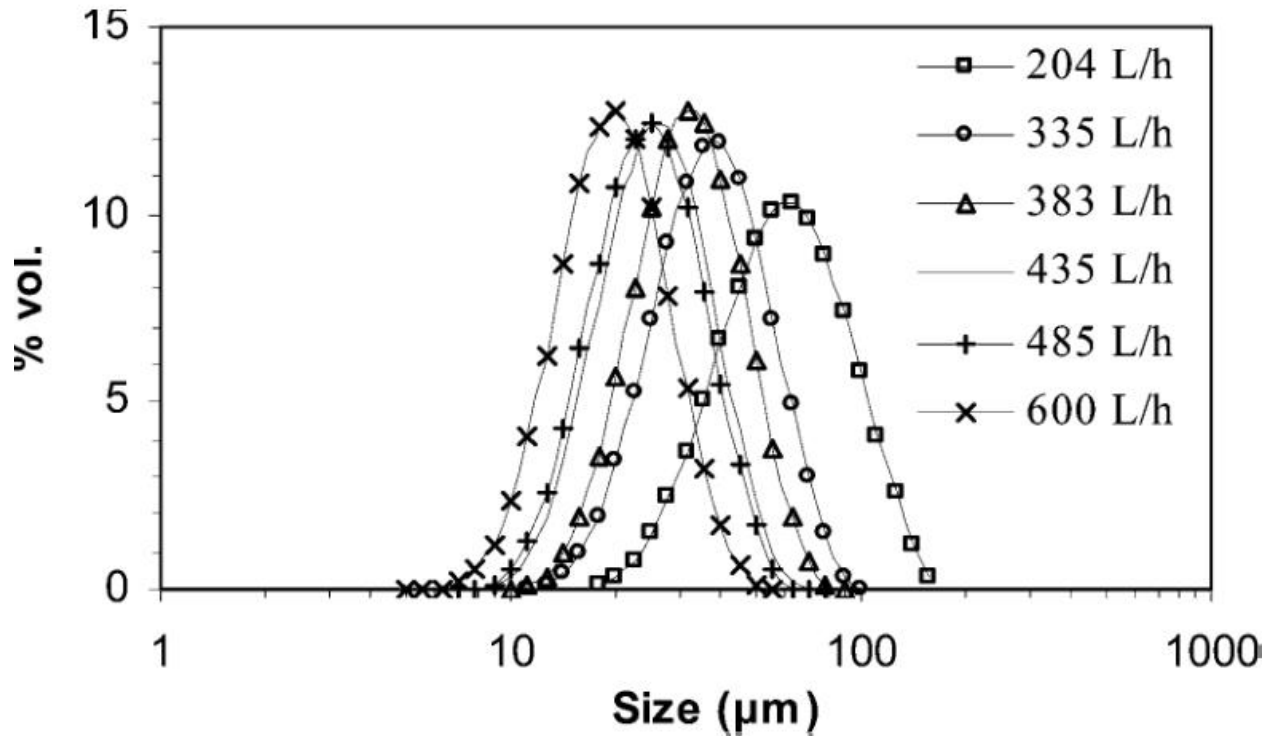


**Figure 2.7** The effect of flow rate on the droplet size distribution in a liquid-liquid dispersion in a 10mm diameter stainless steel tube packed with SMX<sup>®</sup> mixing elements. The fluids used were a water and Tween 80 mixture (aqueous phase) and cyclohexane (organic phase) [9].

Although more accurate measurements of droplet size distribution can be determined experimentally, it would be difficult to justify these experimental works for our study. Instead, we will extrapolate the data to find an estimate for our reactor system. Taking the average droplet size for the various flow rates, we can convert the flow rates to linear velocities and find the relationship between linear velocity and droplet size. The values reported by Theron, namely the average droplet size at each of the six different linear velocities (converted from flow rates),

were plotted and a curve was fitted to this data to represent the relationship between linear velocity and droplet size. This relationship, depicted in Figure 2.8, can be expressed by

$d_p = 105.8e^{(-4 \times 10^{-5}u)}$  where  $d_p$  is the average droplet size and  $u$  is the linear fluid velocity. The average droplet size decays exponential as linear velocity is increased. A high enough linear velocity of the reactants through the PFR must be chosen as to justify the assumption of plug flow. From the linear velocity, we can estimate the average droplet size of the dispersed phase.

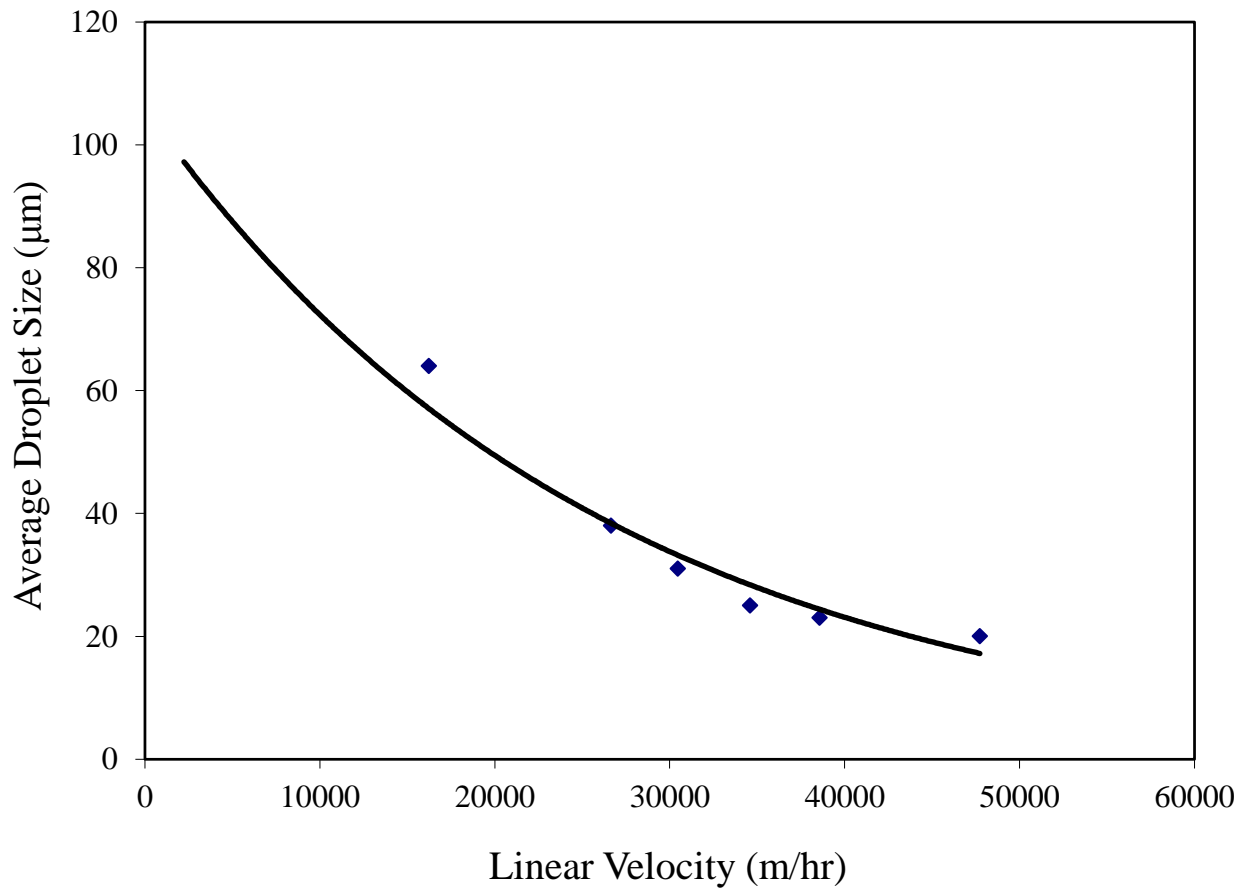


**Figure 2.8** Relationship between linear velocity and average droplet size in a liquid-liquid dispersion. Data reported by Theron (flow rate vs. droplet size) was plotted to find a best fit curve for the linear velocity and droplet size relationship.

Using this droplet size and total volume of the aqueous phase the volume of each droplet, the number of droplets, and specific surface area (surface area of aqueous droplets per cubic meter of total volume),  $a$ , can be calculated. Here we assume that the consumption of BPA from the aqueous phase and the consumption of phosgene from the organic phase will not significantly lower the volume. Therefore, the aqueous phase hold-up (i.e., volume fraction of suspended aqueous liquid droplet phase),  $\Phi_A$ , is constant.  $\Phi_A$  can be expressed as

$$\Phi_A = \frac{N \cdot V_{drop}}{V_{mixture}} \quad (1)$$

where  $N$  is the number of droplets,  $V_{drop}$  is the volume of each droplet, and  $V_{mixture}$  is the total reaction volume. Because the volume of the aqueous phase is assumed to be constant, there is an inverse relationship between the number of droplets and the volume of each droplet. From the average droplet diameter we can calculate the volume of each droplet, and since the aqueous phase hold-up is constant, we can calculate the number of droplets, which is also constant. The specific surface area,  $a$ , is the surface area of the aqueous droplets per unit volume of the mixture and can be calculated as

$$a = \frac{N \cdot 4\pi \left( \frac{d_p}{2} \right)^2}{V_{mixture}} \quad (2)$$



## 2.5 Derivation of Model Equations

A mathematical model of a continuous plug flow reactor for a two phase mixture is now derived for the interfacial process in a tubular reactor. We assume a pseudo-steady state for mass transfer and reaction at the interface. That is, we assume that the amount transferred to the interface is equal to the amount that is consumed at the interface for both phosgene and di-sodium Bisphenate. Further, we assume that the rate of BPA consumption at the interface is equal to the rate of consumption of phosgene at the interface.

The mass transfer rate of phosgene ( $B_o$ ) and di-sodium Bisphenate ( $A_o$ ) can be expressed by the following equations:

$$r_{B_o,m} = -k_{L1}a([B_o] - [B_o^*]) \quad (3)$$

$$r_{A_o,m} = -k_{L2}a([A_o] - [A_o^*]) \quad (4)$$

where  $k_{L1}$  is the mass transfer coefficient of phosgene,  $[B_o]$  is the bulk concentration of phosgene,  $[B_o^*]$  is the interface concentration of phosgene,  $k_{L2}$  is the mass transfer coefficient of di-sodium Bisphenate,  $[A_o]$  is the bulk concentration of di-sodium Bisphenate,  $[A_o^*]$  is the interface concentration of di-sodium Bisphenate, and  $a$  is the specific surface area of the interface between the aqueous and organic phases. Then, the consumption rate of phosgene and di-sodium Bisphenate at the interface by the reaction can be expressed by the following equation:

$$-r_p = -4k_1[B_o^*][A_o^*] \quad (5)$$

As you can see, the rate of reaction of phosgene depends on the concentration of BPA and phosgene at the interface and the kinetic rate constant of this reaction. Also, looking at Equation 5, we see a coefficient of 4. This coefficient comes from the four reaction routes between BPA and phosgene. The two reactive end groups of BPA can react with the two end groups of phosgene for a total of four possible reaction routes. Assuming a quasi-steady state for mass transfer and reaction, we can set each mass transfer rate equal to the consumption rate such that, for phosgene,

$$k_{L1}a([B_o] - [B_o^*]) = 4k_1[B_o^*][A_o^*] \quad (6)$$

Solving for  $[B_o^*]$ , we obtain the following equation for the concentration of phosgene at the interface.

$$[B_o^*] = \frac{k_{L1}a[B_o]}{k_{L1}a + 4k_1[A_o^*]} \quad (7)$$

For the concentration of di-sodium Bisphenate at the interface, we get

$$[A_o^*] = \frac{k_{L2}a[A_o]}{k_{L2}a + 4k_1[B_o^*]} \quad (8)$$

The continuous reactor model is now derived. Let us consider a plug flow reactor segment shown in Figure 2.6. Here, we assume that phosgene is present only in the bulk organic phase (i.e., complete dissolution of phosgene in methylene chloride in upstream tube sections) and that aqueous droplets are dispersed uniformly in the organic phase. The overall fluid velocity is assumed to be constant at  $u$  along the reactor length. It is also assume that both the organic

phase and the aqueous droplet phase move at the same speed through the reactor. Then, the non-steady state mass balance equation for phosgene is derived as follows:

$$\frac{\partial(A\Delta z\Phi_B[B_o])}{\partial t} = uA\Phi_B[B_o]_{|_z} - uA\Phi_B[B_o]_{|_{z+\Delta z}} - A\Delta z\Phi_B \begin{bmatrix} k_L a([B_o] - [B_o^*]) - 4k_2[A][B_o] \\ -2k_3[B_o][P_o] \end{bmatrix} \quad (9)$$

Since the cross sectional area,  $A$ , and  $\Phi_A$  are constant, equation (9) is reduced to

$$A\Phi_B \frac{\partial([B_o])}{\partial t} = -uA\Phi_B \frac{\partial[B_o]}{\partial z} - A\Phi_B [k_L a([B_o] - [B_o^*]) - 4k_2[A][B_o] - 2k_3[B_o][P_o]] \quad (10)$$

The term  $A\Phi_A$  can be removed from the expression. At steady state,  $\frac{\partial[B_o]}{\partial t} = 0$ . Then, the

concentration profile for phosgene is as follows.

$$u \frac{d[B_o]}{dz} = -k_L a([B_o] - [B_o^*]) - 2k_2[A][B_o] - 2k_3[B_o][P_o] \quad (11)$$

Similarly, the model equations of BPA and all intermediate and polymeric species are derived from the reaction kinetics for each species assuming a steady state process.

The following is a list of all the rate equations for this model.

$$u \frac{d[B_o]}{dz} = -k_L a([B_o] - [B_o^*]) - 2k_2[A][B_o] - 2k_3[B_o][P_o] \quad (12)$$

$$[B_o^*] = \frac{k_{L1} a [B_o]}{k_{L1} a + 4k_1 [A_o^*]} \quad (13)$$

$$u \frac{d[A_o]}{dz} = -k_L a ([A_o] - [A_o^*]) \quad (14)$$

$$[A_o^*] = \frac{k_{L2} a [A_o]}{k_{L2} a + 4k_1 [B_o^*]} \quad (15)$$

$$u \frac{d[A]}{dz} = \begin{bmatrix} 4k_1 [A_o^*] [B_o^*] - 2k_2 [A] [B_o] - 2k_1 [A] [B] - 2k_1 [A] [A] - k_3 [A] [P_o] - k_3 [A] [P_1] \\ -k_1 [A] [Z_1] - k_1 [A] [Z_2] \end{bmatrix} \quad (16)$$

$$u \frac{d[B]}{dz} = 2k_2 [A] [B_o] - 2k_1 [B] [A] - 2k_3 [B] [P_o] - 2k_1 [B] [Z_1] \quad (17)$$

$$u \frac{d[P_o]}{dz} = -2k_3 [P_o] [B_o] - k_3 [P_o] [A] - 2k_3 [P_o] [B] - k_3 [P_o] [Z_2] \quad (18)$$

$$u \frac{d[P_1]}{dz} = 2k_3 [P_o] [B_o] - k_3 [P_1] [A] - k_3 [P_1] [Z_1] \quad (19)$$

$$u \frac{d[P]}{dz} = k_3 [P_1] [Z_1] + k_3 [P_o] [Z_2] \quad (20)$$

$$u \frac{d[Z_1]}{dz} = \begin{bmatrix} 2k_1 [A] [A] - k_1 [Z_1] [A] - 2k_1 [Z_1] [B] + k_1 [Z_1] [A] + k_3 [A] [P_o] - k_3 [Z_1] [P_1] \\ -k_1 [Z_1] [Z_2] \end{bmatrix} \quad (21)$$

$$u \frac{d[Z_2]}{dz} = \begin{bmatrix} 2k_1 [A] [A] + 2k_1 [A] [B] + 2k_1 [A] [B] - k_1 [Z_2] [A] + k_1 [Z_2] [A] + 2k_1 [B] [Z_1] \\ + k_3 [A] [P_1] + 2k_3 [B] [P_o] - k_3 [Z_2] [P_o] - k_1 [Z_1] [Z_2] \end{bmatrix} \quad (22)$$

The initial conditions for equations (12), (14), (16)-(22) are given as follows:

$$B_o(0) = 1.0, A_o(0) = 0.35, P_o(0) = 0.05, A_o^*(0) = B_o^*(0) = A(0) = B(0) = P_1(0) = P(0) = Z_1(0) = Z_2(0) = 0$$

Please note that the initial conditions are normalized and dimensionless due to the proprietary nature of the experimental data.

Here, we assume that the chain length of polymeric species does not affect the reactivity of its end groups (i.e. the rate constants do not change during the interfacial process). Further, the case considered in this study assumes that the phase equilibrium constants (mass transfer coefficients) are independent of pressure and are linearly correlated to the composition.

## 2.6 Tubular Reactor Schematic

The model equations derived in the previous section are solved for the tubular reactor system depicted in Figure 2.9. Phosgene gas enters the reactor and is mixed with methylene chloride (solvent) in Zone A, upstream of the tubular reactor. Phosgene gas is assumed to be completely dissolved in the organic solvent. A caustic aqueous solution of BPA ( $H_2O$ ,  $NaOH$ , and BPA) is then added to the phosgene-solvent mixture and the entire two-phase feed mixture is injected into the reactor. There are two additional ports along the tubular reactor for the side feeds of reactants or additives such as chain stoppers. The two-phase mixture passes through a stack of static mixing elements packed in the reactor and fine aqueous droplets are generated and flow with the bulk organic phase. The chain stopper (PTBP) is added at injection point 2 for control of the molecular weight. Finally, at injection point 3, additional sodium hydroxide ( $NaOH$ ) can be introduced to the reactor to maintain the pH at around 12. The pressure (85 PSI) and temperature ( $35^{\circ}C$ ) are maintained constant in the reactor. The reactor model presented in the previous section applies to the main tubular reactor zone.

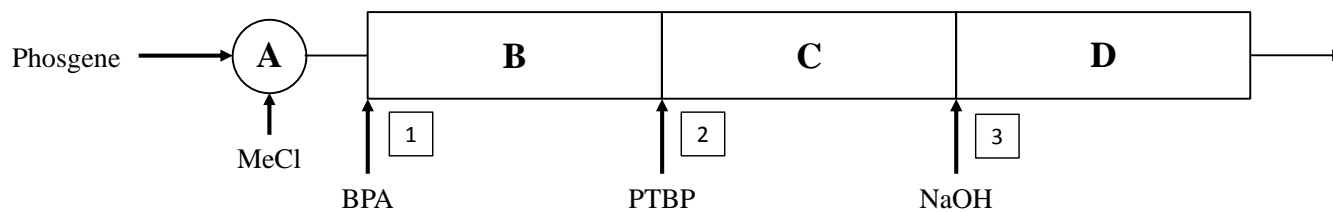


**Figure 2.9** Tubular Reactor System Schematic

## 2.7 Parameter Estimation

The fidelity of a model is strongly dependent on the parameter values. We have adopted the literature values of the kinetic parameters for the reactor simulations. Table 2.3 shows the initial estimates of the six major parameters used in the model equations.

**Table 2.3** Model Parameters Initial Estimates

Model Parameters	Values	Reference
$k_1$ (rate constant for polymerization)	$8.6 \times 10^{-4} \text{ m}^3/\text{mol sec}$	[6] Mills P.
$k_2$ (rate constant for bulk phosgene)	$1.5 \times 10^{-5} \text{ m}^3/\text{mol sec}$	Estimated
$k_3$ (rate constant for PTBP)	$1.5 \times 10^{-5} \text{ m}^3/\text{mol sec}$	Estimated
$k_{L1}$ (mass transfer coefficient of phosgene)	$1.33 \times 10^{-5} \text{ m/sec}$	[10] Yaws
$k_{L2}$ (mass transfer coefficient of BPA)	$1.6 \times 10^{-5} \text{ m/sec}$	Estimated

The value of  $k_1$ , the kinetic rate constant for polymerization reactions (BPA and phosgene), was estimated using the values for the propagation rate constant presented in the literature [6]. The two values for the propagation rate constant that were used in the simulation model by Mills were 0.01 and  $1.0 \times 10^{-4} \text{ m}^3/\text{mol sec}$ , respectively. The initial value set for  $k_1$  was  $0.001 \text{ m}^3/\text{mol sec}$  and was adjusted to  $8.6 \times 10^{-4} \text{ m}^3/\text{mol sec}$  to match the number average molecular weight data from the plant. The mass transfer coefficient for phosgene was approximated using a Sherwood Number of 2, which will give a very conservative estimate of the mass transfer coefficient.

$$\begin{aligned}
Sh = 2 &= \frac{k_L \cdot d_p}{D} & (23) \\
D &= 6 \times 10^{-10} \text{ m}^2 / \text{sec} \\
d_p &= 9 \times 10^{-5} \text{ m} \\
\therefore k_L &= 1.33 \times 10^{-5} \text{ m / sec}
\end{aligned}$$

In Yaws' Transport Properties of Chemicals and Hydrocarbons [10], Yaws reports that the diffusion coefficient of phosgene ( $D$ ) in water is  $6.0 \times 10^{-10} \text{ m}^2/\text{sec}$  at  $25^\circ\text{C}$ , which is very close to the reaction temperature.  $d_p$  is the diameter of the aqueous droplet size. Due to an absence of kinetic data for PTBP in this system, the kinetic rate constant for PTBP was assigned a value such that the conversion of PTBP is nearly 100%.

We used a total of four proprietary plant data sets from industry for the interfacial process in this tubular reactor system. Due to the proprietary nature of the plant data, we are not able to show the actual data and thus we shall use the normalized plant data in this thesis. The normalized data is shown in the Table 2.4. Using this set of data, we have optimized the model parameters, using a MATLAB optimization protocol, to fine-tune the model and improve its accuracy significantly. Using the initial estimates of these parameters, the optimization protocol adjusts the parameters such that the error between the experimental values ( $M_n$ , polymer production rate) and the simulated values is minimized. Table 2.5 lists the optimized parameter values.



**Table 2.4** Proprietary Plant Data for Interfacial Process in Tubular Reactor (Normalized)

	Grade 1	Grade 2	Grade 3	Grade 4
<b>Polymer Production Rate (kg/hr)</b>	0.73	0.92	0.73	1.0
<b>Mw</b>	1.0	0.71	0.66	0.52
<b>Mn</b>	1.0	0.68	0.65	0.53

**Table 2.5** Optimized Parameter Values

Parameters	Definition	Optimized Value
$k_1$	Kinetic Rate Constant for Polymerization	$9.58 \times 10^{-5} \text{ m}^3/\text{mol sec}$
$k_2$	Kinetic Rate Constant for CDC Reaction in Bulk Phase	$2.24 \times 10^{-6} \text{ m}^3/\text{mol sec}$
$k_3$	Kinetic Rate Constant for PTBP	$7.20 \times 10^{-6} \text{ m}^3/\text{mol sec}$
$d_p$	Dispersed Aqueous Drop Diameter	$4.62 \times 10^{-6} \text{ m}$
$k_{L1}$	Mass Transfer Coefficient of CDC	$2.71 \times 10^{-5} \text{ m/sec}$
$k_{L2}$	Mass Transfer Coefficient of BPA	$9.00 \times 10^{-7} \text{ m/sec}$

The MATLAB protocol that was used is called “fminsearch” which can be used to find the minimum of a scalar function of several variables starting at an initial estimate. This protocol is an unconstrained nonlinear optimization. The function used in this protocol was our homopolymerization model and the variables were the 6 parameters listed in Table 2.1. The number of iterations for this protocol can be set to a desired value. With the previously reported parameter values as initial estimates, this protocol implements the function (homopolymerization model) for the four different grades of polycarbonate (Table 2.3) and calculates the average error between experimental and calculated values for the average molecular weight and polymer production rate for the four grades of PC. Then, the parameter values are slightly adjusted, for each iteration, to minimize this error.

The fminsearch protocol was used with an iteration value of 500 initially. At the end of the 500 iterations, the optimized parameter values were set as the new initial values, and the protocol was implemented again. This procedure was repeated until the minimum error was reached, which was the point at which the error value did not decrease further.

Using this optimization protocol, our homopolymerization model was optimized and the results are discussed in the following section.

## 2.8 Simulation Results

Using the simulation model, we can predict the concentration profiles and molecular weight profiles in the tubular reactor. The figures below depict the output from the model in graphical form. The axial distance is given in dimensionless form and the concentrations have been normalized by dividing the data values by an appropriate number for each set of data shown in the following figures.

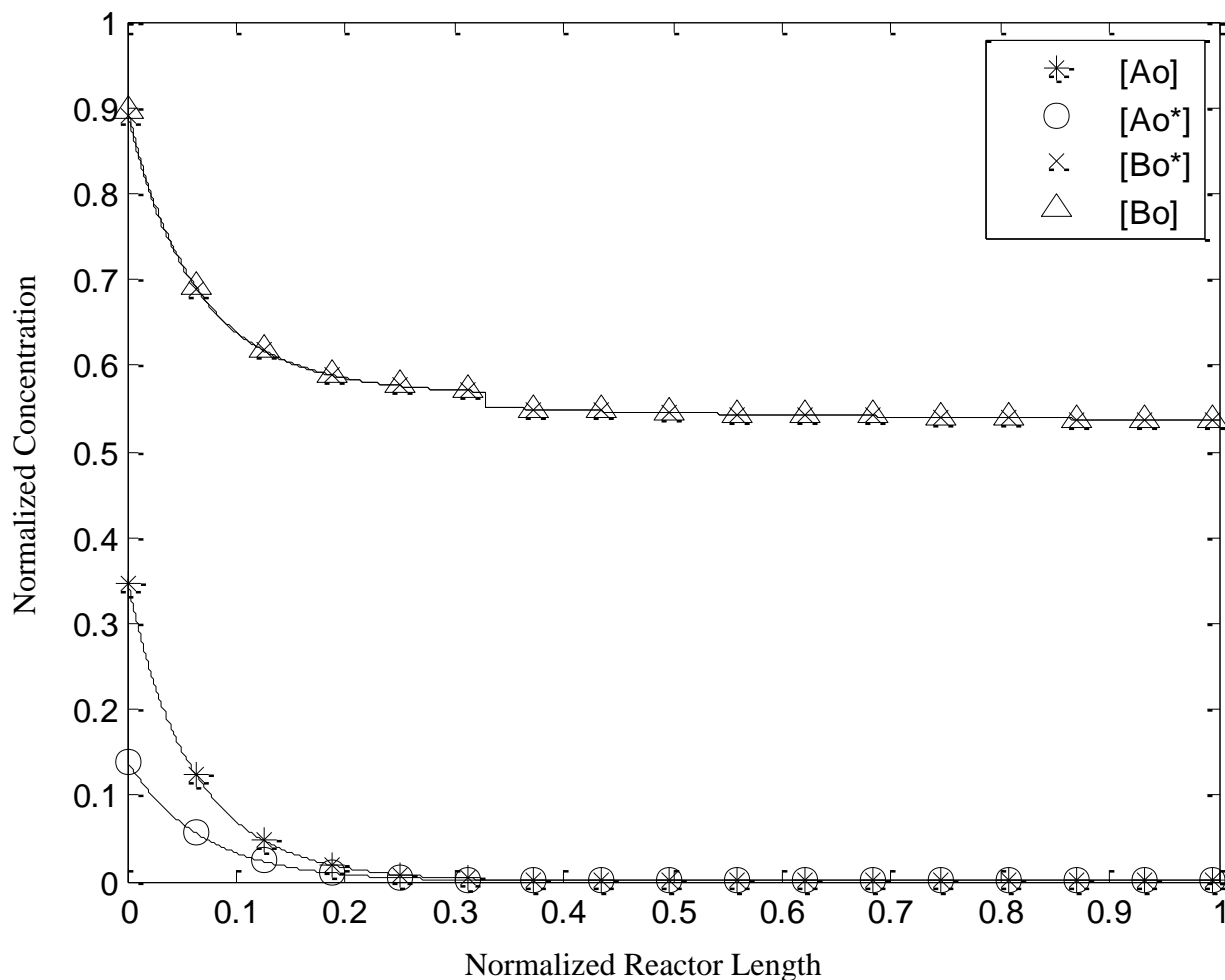


**Figure 2.10** Normalized concentration profiles for the BPA in the aqueous phase ( $A_o$ ), BPA at the interface ( $A_o^*$ ), phosgene in the organic phase ( $B_o$ ), and phosgene at the interface ( $B_o^*$ ). Simulation results.

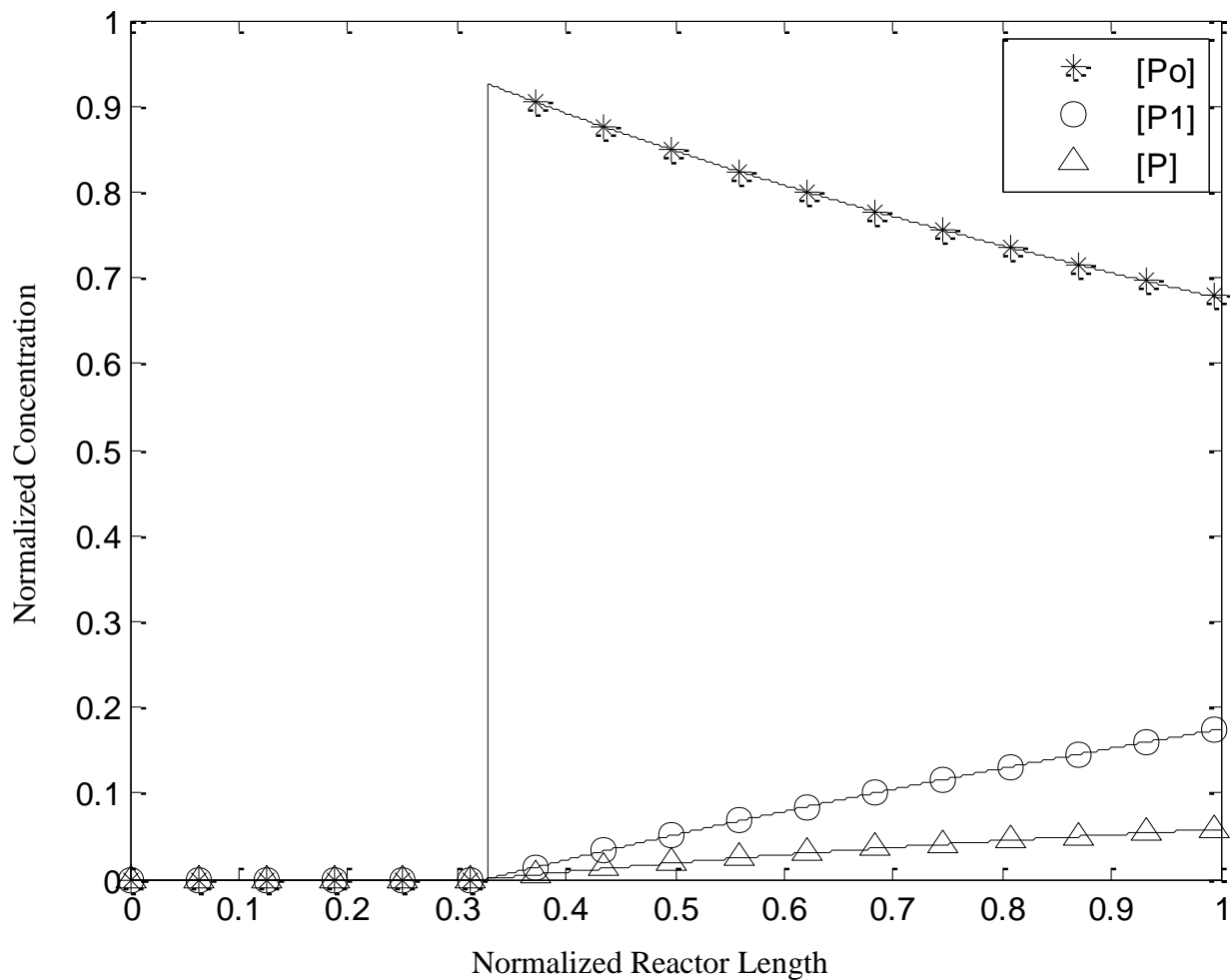


**Figure 2.11** Normalized concentration profiles for para-tertiary butyl phenol ( $P_0$ ), modified para-tertiary butyl phenol ( $P_1$ ), and end-capped species ( $P$ ). Simulation results.

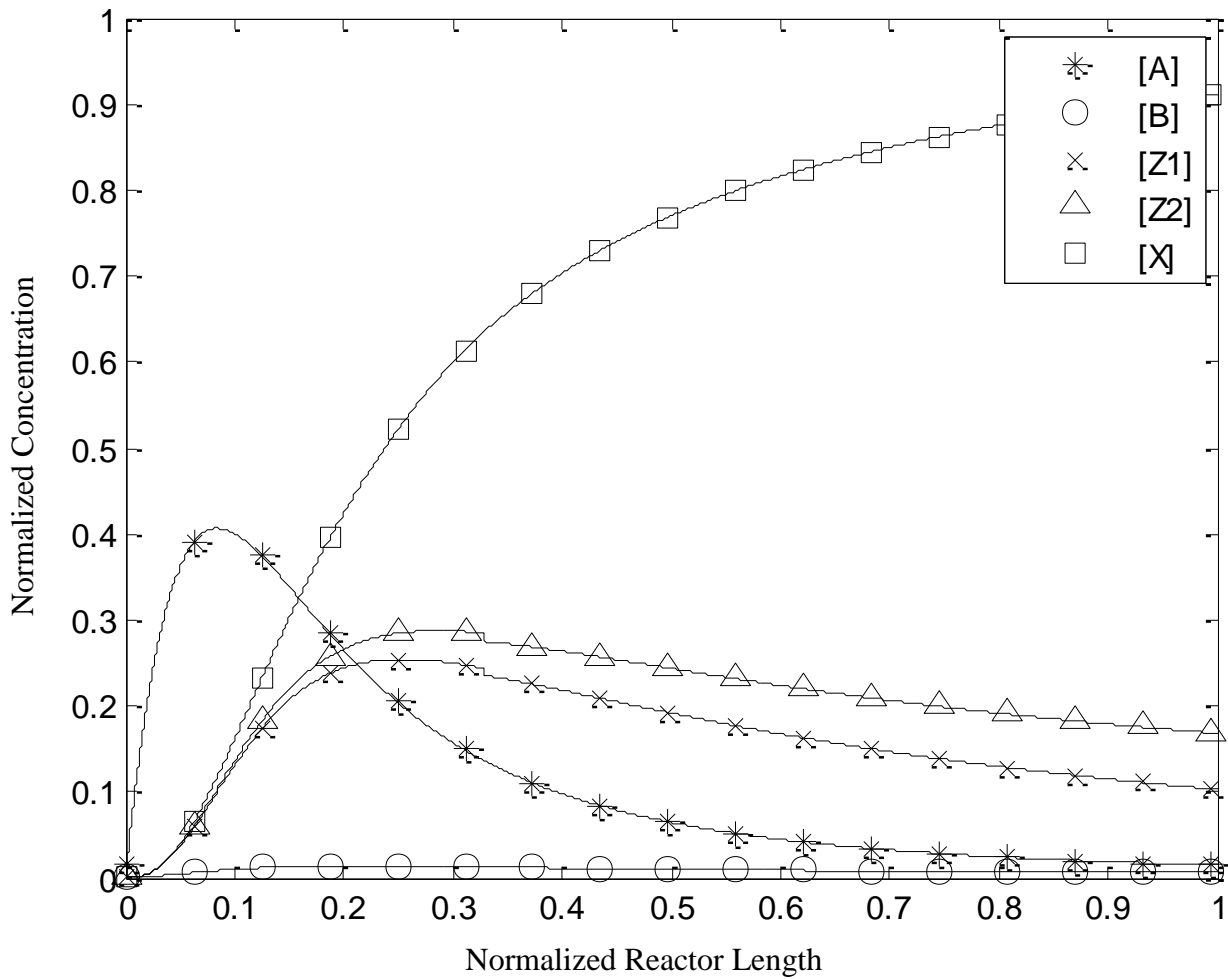


**Figure 2.12** Normalized concentration profiles for intermediate species: monochloroformate (A), bischloroformate (B); polymeric species: Z<sub>1</sub>, Z<sub>2</sub>; and carbonate linkages (X). Simulation results.

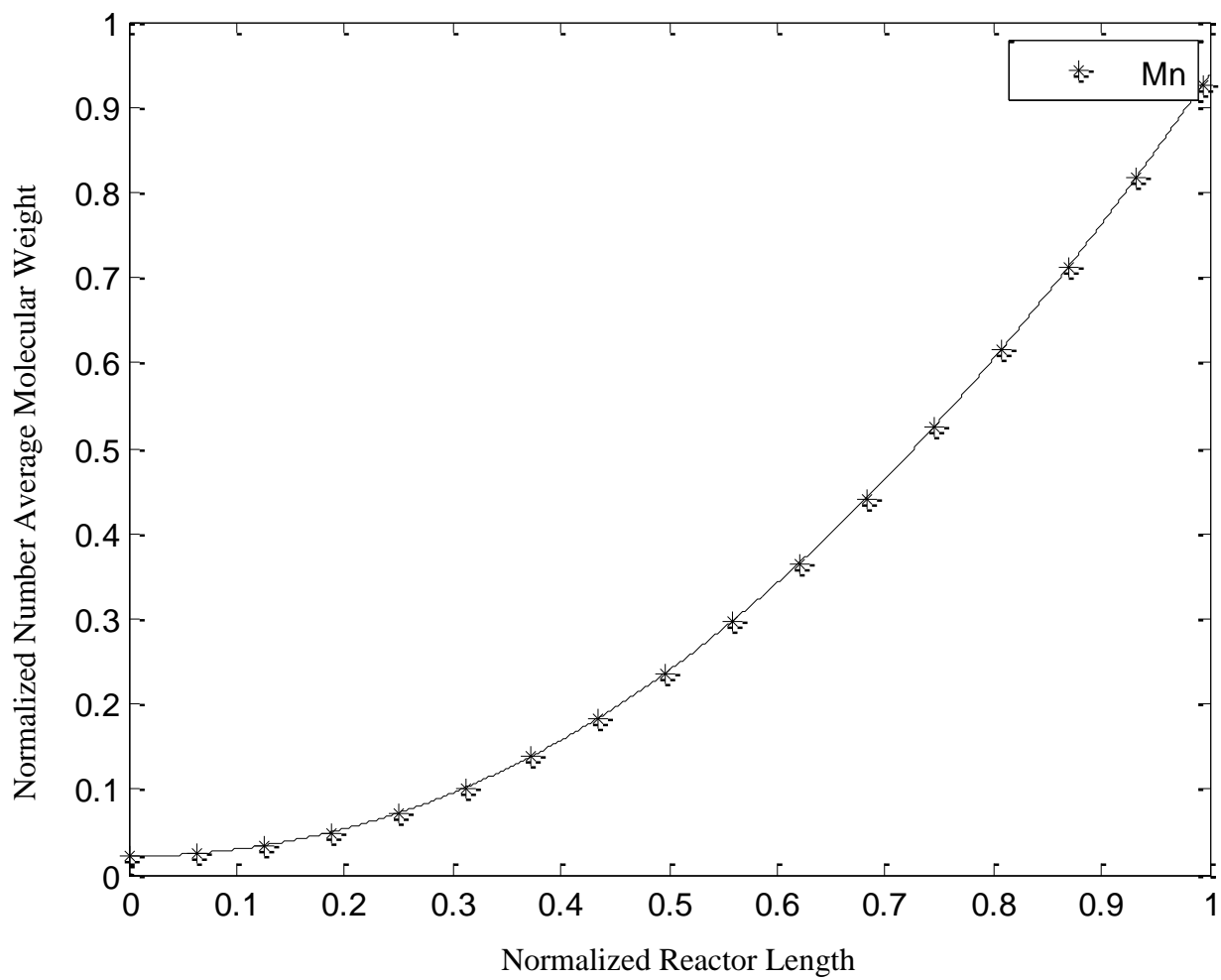


**Figure 2.13** Evolution of normalized number average molecular weight ( $M_n$ ). Simulation results.

Figures 2.10-2.13 show that the simulation model predictions are very satisfactory. Figure 2.10 shows the consumption rate of monomers (BPA and phosgene). Since this system is a step-growth process, we would expect the consumption rates of both monomers to be very similar. It is interesting to note that, for both monomers, the interface concentrations coincide with the bulk phase concentrations throughout the majority of the process as can be seen in Figure 2.10. Also in Figure 2.10, The mass transfer resistance of phosgene can be seen as insignificant in the mass transfer and reaction process at the interface as the both phosgene concentrations are identical. The mass transfer resistance of BPA is greater than that of phosgene. The mass transfer coefficient of BPA is  $9.00 \times 10^{-7}$  m/sec and the mass transfer coefficient of phosgene is  $2.71 \times 10^{-5}$  m/sec. Thus, we see that the interface BPA concentration is slightly lower than the bulk BPA concentration. As discussed previously, we have assumed a quasi-steady state for the mass transfer and reaction at the interface. This is a reasonable result considering that we assume the rate of mass transfer to the interface is equivalent to the rate of consumption via reaction. Further, Figure 2.11 shows that as the reaction progresses, PTBP is consumed and end-capped units are produced. Figure 2.12 depicts the concentration profiles for intermediate and polymeric species. We can see that carbonate linkages (X) is steadily produced throughout the process. However, the monomer consumption rate becomes negligible after about the first third of the process. After this point, even though BPA and phosgene consumption rates are close to zero, the chloroformates and oligomers/polymers continue to react in the organic phase increasing the number average molecular weight, seen in Figure 2.13. In fact, the molecular weight grows more in the latter half of the process due to these reactions. The

comparisons between the experimental data and predicted values are summarized in the following table.

**Table 2.6** Experimental vs. Predicted Results for  $M_n$  and Polymer Production Rate (Normalized)

	<b>Mn</b> <b>(Experimental)</b>	<b>Mn</b> <b>(Model)</b>	<b>Production Rate</b> <b>(Experimental)</b>	<b>Production Rate</b> <b>(Model)</b>
<b>Grade 1</b>	1.00	0.97	0.73	0.74
<b>Grade 2</b>	0.68	0.62	0.92	0.91
<b>Grade 3</b>	0.65	0.65	0.73	0.66
<b>Grade 4</b>	0.53	0.58	1.00	0.97

Figure 2.14 depicts this comparison in graphical form. By plotting the experimental values vs. the values predicted by the model, we see that all the data points are very close to the 45 degree line indicating that the error is minimal. In fact, the model predicts the number average molecular weight within the average error of 2 chain lengths (~500g/mol) and the polymer production rate within the average error of about 3%.



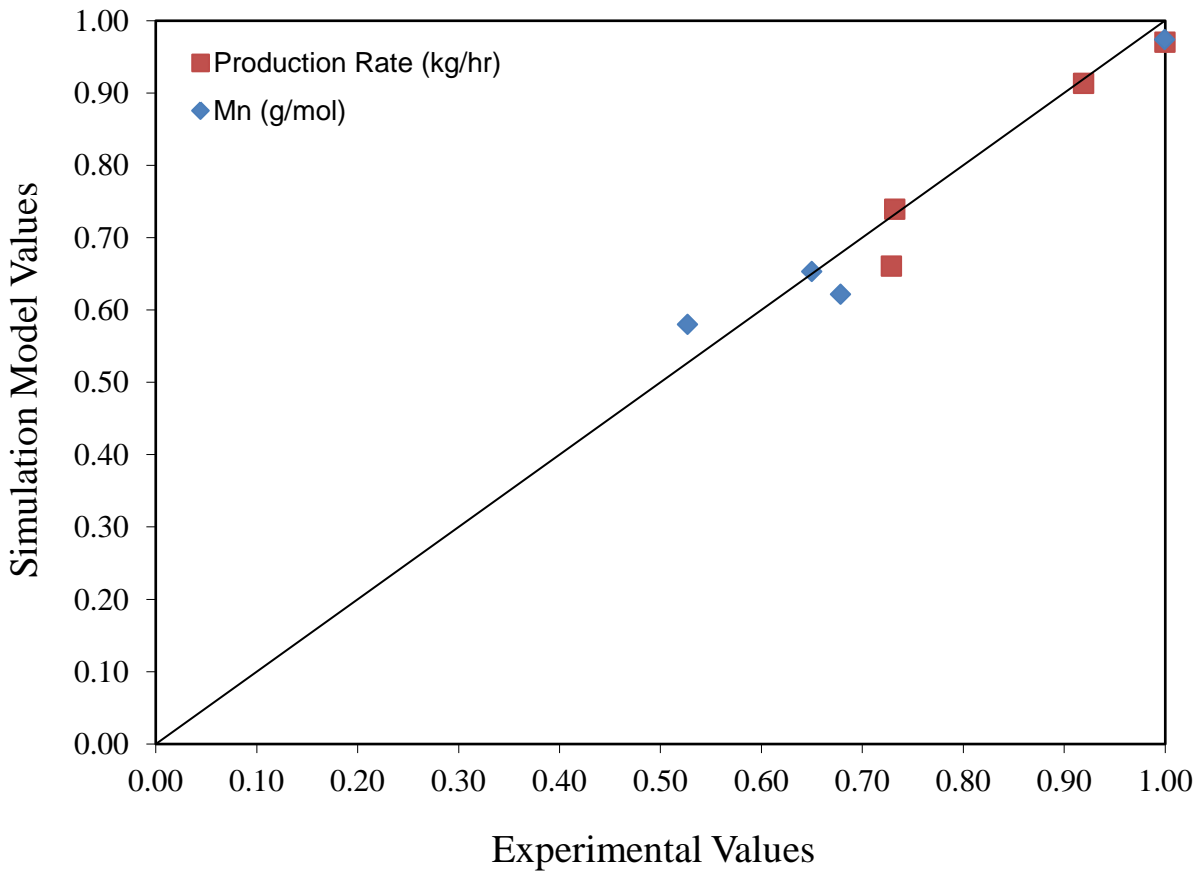


**Figure 2.14** Comparison of experiment and predicted values of number average molecular weight and polymer production rate.

## 2.9 Polymer Chain Length Distribution

Molecular weight distribution (or chain length distribution) is a very important property that can affect the physical properties of the polymer. Even if two polymer samples have the same average molecular weight, they may have different chain length distributions which can lead to different polymer rheology and different end user properties. Thus, being able to calculate the chain length distribution in the model can be significant.

For A-B type polycondensation or A-A + B-B type polycondensation with equimolar amounts of A-A and B-B type monomers, Flory's most probable distribution is a good estimate of the chain length distribution. There are two parameters for Flory's distribution function,  $x$  and  $p$ :  $x$  is the chain length and  $p$  is the extent of reaction. Flory's distribution function in terms of weight fraction of  $x$ -mer ( $W_x$ ) is as follows [11].

$$W_x = xp^{(x-1)}(1-p)^2 \quad (24)$$

Flory's distribution can also be expressed in terms of number fraction of  $x$ -mer ( $N_x$ ).

$$N_x = N_o p^{(x-1)}(1-p)^2 \quad (25)$$

$N_o$  is the initial number of moles of both monomers.  $p$  is the extent of reaction (conversion) of a functional reactive end group. For example, the conversion  $p$  for BPA is defined as,

$$p = \frac{[A_o(0) + A(0) + B(0)] - [A_o + A + B]}{[A_o(0) + A(0) + B(0)]} \quad (26)$$

where  $A_o(0)$ ,  $A(0)$ , and  $B(0)$  are the initial concentrations of BPA, species A and species B, respectively (See Figures 2.5 and 2.6). BPA is denoted by  $A_o$ . Also, we must consider species A and B as well. A and B are BPA units that have reacted with phosgene at the interface, having different end groups as a result; A has chloroformate groups on both ends while B has one hydroxyl group and one chloroformate group ( $A(0)=B(0)=0$ ). Furthermore, A and B are species that have not been added to the polymer chain and has no effect on chain length. Thus, to see the overall conversion of BPA, we must consider all three species.

Using Flory's distribution theory, we can calculate the chain length distribution of polymers at any point in the reactor. For brevity, we only consider the distributions at the end of Zone B, at the end of Zone C, and at the end of Zone D. It is noted that no matter how a condensation polymer is formed, they will end up with a distribution resembling Flory's most probable distribution. Figure 2.15 shows the calculated polymer weight chain length distribution curves at three different reactor positions.

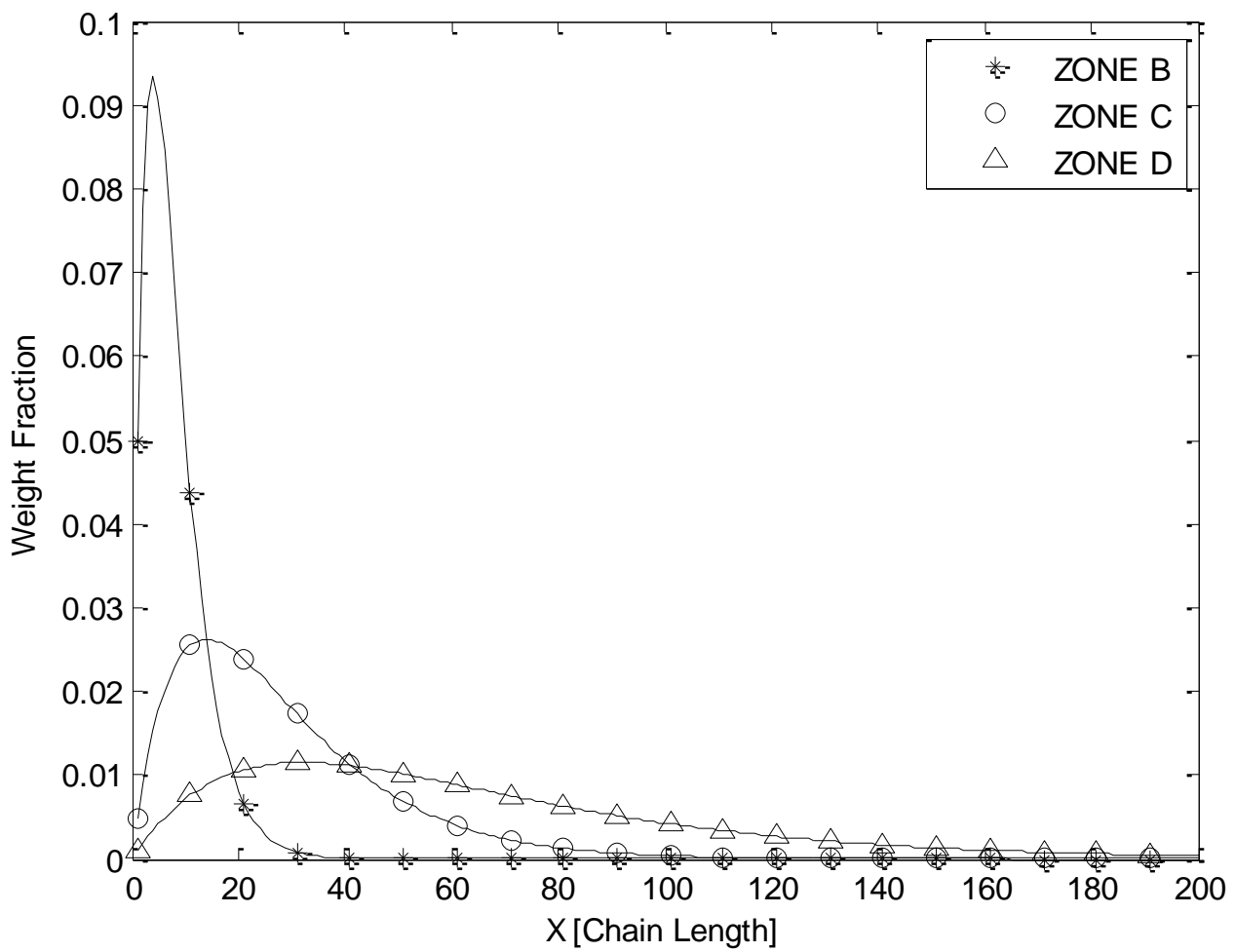


**Figure 2.15** Flory's most probable distribution at three different positions along the tubular reactor (Zone B, Zone C, Zone D). Simulation results.

As expected, the average chain length of the polymer increases as the reaction progresses. The polydispersity increases as the reaction progresses as well. The results presented in Figure 2.15 do not show anything particularly unusual.

We know that the number average molecular weight is given by

$$M_n = \frac{\sum_i N_i M_i}{\sum_i N_i} \quad (27)$$

where  $N_i$  is the number fraction of i-mers and  $M_i$  is the molecular weight of i-mers. Using equation (27) and the number chain length distribution from Figure 2.15, we can calculate the number average molecular weight and compare the values to the results we get from the phosgene process model simulation.

**Table 2.7** Normalized average molecular weight (Flory Distribution vs. Simulation results)

<b>Normalized Reactor Length</b>	<b><math>M_n</math> (Distr.)</b>	<b><math>M_n</math> (Model)</b>
0.33	0.11	0.12
0.65	0.34	0.42
1.00	0.76	1.00

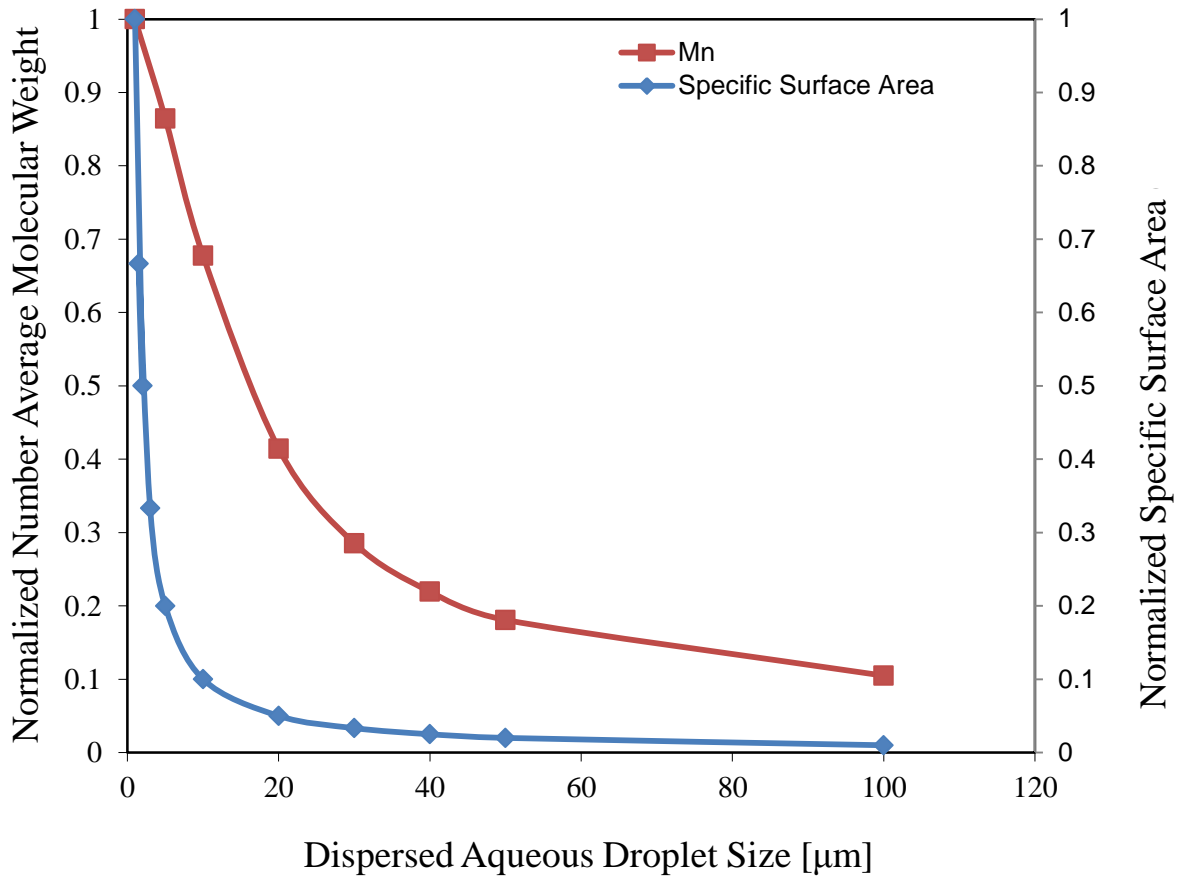
Table 2.7 shows the values of the number average molecular weight at the three zones along the PFR. The error between the average molecular weight calculated by solving the model equations and by using Flory's distribution is approximately 18%. This error, while not insignificant, shows that Flory's distribution theory fairly accurately predicts the actual chain length distribution. The error can be attributed to the fact that Flory's distribution function does not account for the mass transfer processes that occur in this system. Flory's distribution theory utilized here assumes an equimolar concentration of the two monomers. In this system, there is an excess of phosgene (about 5:1 molar ratio of phosgene to BPA). However, the reaction between phosgene and BPA occurs at the interface where we have assumed a pseudo-steady state for mass transfer and reaction, meaning that the rate of consumption at the interface equals the rate of mass transfer to the interface for both phosgene and BPA. Our assumption further implies that, even though there exists an excess of phosgene in the bulk organic phase, at the interface, the consumption rate of BPA and phosgene are equal. Thus, the mass transfer rate of each monomer to the interface is equal (i.e. the concentration of BPA and phosgene at the interface can be considered equimolar for the purposes of calculating the chain length distribution). Moreover, we have seen from simulation model results (Figure 2.10) that the interface and bulk concentration of both monomers are very similar. We can see that the number average molecular weights, calculated from Flory's Distribution along the PFR, are a good match with the predicted number average molecular weights from the simulation model. Thus, our assumption of a pseudo-steady state at the interface is confirmed.

## 2.10 Effect of Bisphenol A Mass Transfer Rate on Polymer Properties

We have established an accurate simulation model of the interfacial process in a tubular reactor. Using this model, we can study the dynamics of this heterophase system. We have seen that the assumption of a quasi-steady state for the mass transfer and reaction at the interface is quite reasonable for this system and have determined that the mass transfer resistance of phosgene is insignificant. However, the mass transfer process plays a significant role because it affects the availability of BPA at the interface. By varying the reactor parameters in the model, the influence of the mass transfer rate on the interfacial process can be investigated. The mass transfer rate of monomers from their respective bulk phases to the interface depends on the difference between the bulk and interface concentration of each monomer. Other parameters that would heavily affect the rate of mass transfer are the total surface area available for mass transfer and the mass transfer coefficient. This surface area is determined by size of the dispersed aqueous droplets assuming that the aqueous phase liquid hold-up remains constant (Equation 2). We have investigated the effect of the dispersed aqueous droplet size and BPA mass transfer coefficient on the number average molecular weight obtainable.

Figure 2.16 shows that the relationship between drop size and molecular weight exhibits an exponential decay (as droplet size increases, the molecular weight decreases). With the same liquid hold-up of the aqueous phase, varying the dispersed aqueous droplet size significantly affects the specific surface area (surface area to volume ratio) and thus the rate of mass transfer. The total surface area available for mass transfer decreases when the droplet size increases. Thus, with larger average droplet diameters, the availability of BPA for reaction at the interface decreases due to the slower mass transfer rate of BPA. With lower concentrations of BPA at the

interface, the reactions at the interface have slower rates which ultimately results in lower molecular weights. The effect of aqueous droplet size has a smaller impact at larger diameters. Increasing the diameter from 1 $\mu\text{m}$  to 20 $\mu\text{m}$  results in a 60% decrease in average molecular weight, whereas, increasing the diameter from 50 $\mu\text{m}$  to 100 $\mu\text{m}$  only results in an 8% decrease.





We can also see the effect of the BPA mass transfer coefficient on the average molecular weight in Figure 2.17. For a small mass transfer coefficient (i.e.  $1.0 \times 10^{-7}$  m/s), the average molecular weight of the polymer is quite low. Due to the slow rate of BPA transfer to the interface, the reaction at the interface progresses at a slow rate as well. In this case, the process is diffusion controlled; the reaction rate is quick, but the diffusion rate hinders the rate of polymerization. As the mass transfer coefficient increases, the obtainable molecular weight increases as well. However, after a certain point (a mass transfer coefficient of about  $4.0 \times 10^{-6}$  m/s), we see no increase in molecular weight. At this point, the process is reaction controlled: the diffusion of BPA to the interface is very fast, but the rate of reaction limits the obtainable molecular weight.

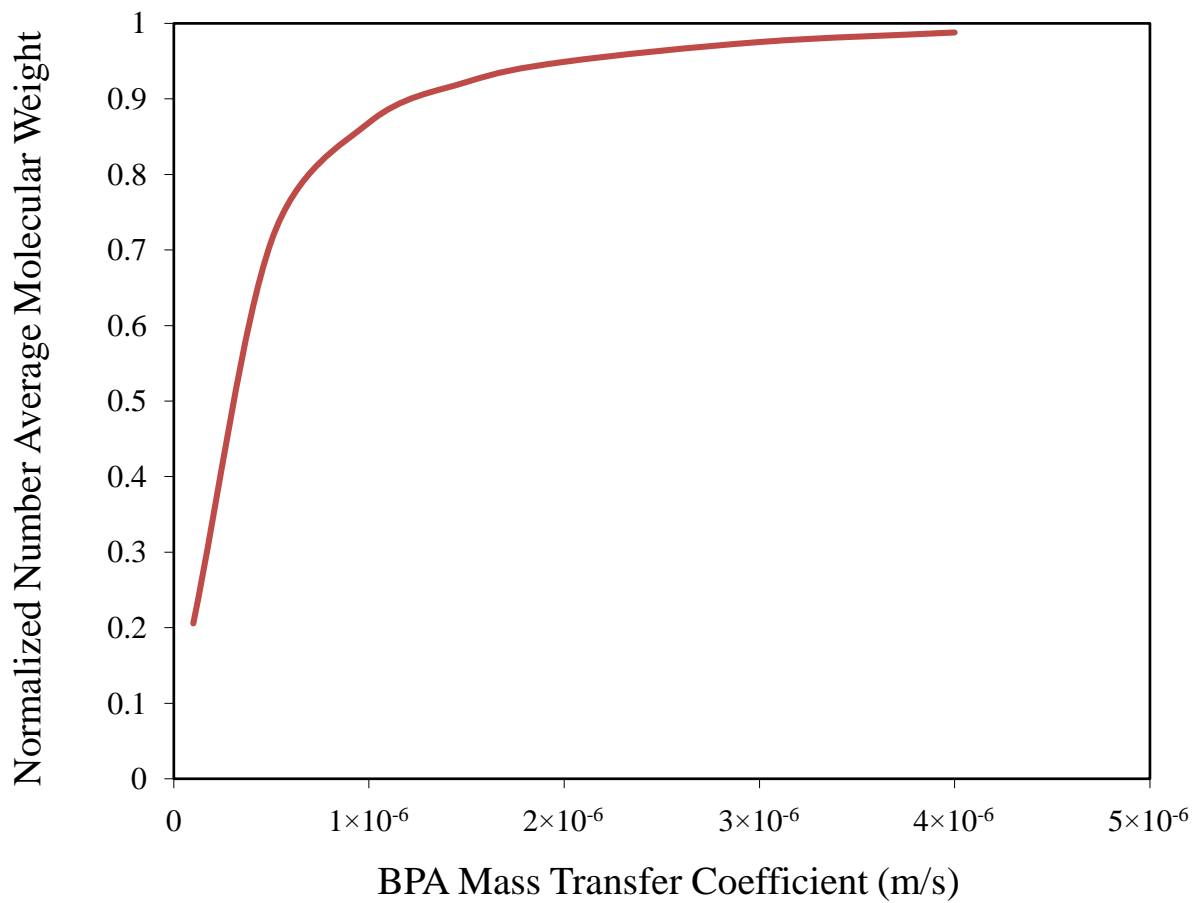


**Figure 2.17** The effect of BPA mass transfer coefficient on the number average molecular weight obtainable. With small mass transfer coefficients, this process exhibits diffusion controlled behavior, while at large mass transfer coefficients, this process exhibits reaction controlled behavior. Simulation Results.

## 2.11 Conclusion

In this chapter, our tubular reactor system and the interfacial process reaction mechanism were discussed in more detail. Further, we defined the reaction scheme by identifying the chemical species involved in the mass transfer and reactions that occur in the bulk phases and at the interface. By doing so, we established the complete set of chemical reactions from which the kinetic model (i.e. simulation model equations) has been derived using a functional group method. It has been determined that the reactor parameters, such as efficacy of mixing and fluid velocity, have a significant impact on the mass transfer process, and ultimately, the reaction kinetics. The parameters of this model (kinetic rate constants and mass transfer rate coefficients) have been optimized using data obtained from an industrial pilot plant of this system. The results of this model, namely the concentration profiles of the reactants, the number average molecular weight, and overall polymer production rate, show a strong fidelity to the actual process, predicting the number average molecular weight within the average error of 2 chain lengths and the polymer production rate within the average error of approximately 3%. We also studied the distribution of chain lengths using Flory's most probable distribution and found that the model predicts the average chain length distribution accurately. Finally, we investigated the effect of the dispersed aqueous droplet size and BPA mass transfer coefficient on the average molecular weight.

## Chapter 3. Copolymerization

### 3.1 Introduction

It has been well known in the literature, especially patent literature, that siloxane-polycarbonate copolymers exhibit excellent thermal stability, good weathering properties and lower glass transition temperatures [12-17]. Polysiloxanes, such as PDMS, can be incorporated into polycarbonate backbone through both the interfacial and melt processes. In the melt process, functionalized siloxanes, such as secondary amine-terminated or carboxylic acid-terminated siloxanes, have been prepared by extrusion with high molecular weight polycarbonates. In the interfacial process, functionalized siloxanes are capped with desired phenolic or acid chloride groups which are then added to the interfacial polymerization reactor with the BPA and phosgene [2]. By incorporating a polysiloxane co-monomer to the functional group model, we can predict the overall siloxane composition and properties of the resulting co-polymer. Siloxane-polycarbonate copolymers exhibit enhanced properties such as solvent resistance, low temperature impact strength, improved processing and flame retardancy.

To the functional group model discussed in Chapter 2, we consider the addition of an additional comonomer, polysiloxane. The following illustrates the examples of siloxane comonomers used for the synthesis of copolycarbonates.

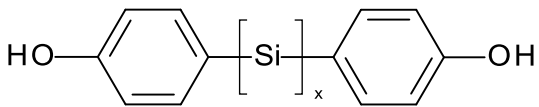
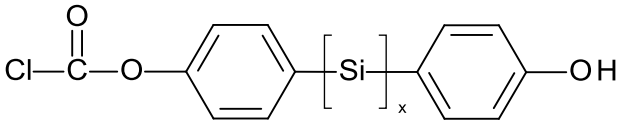
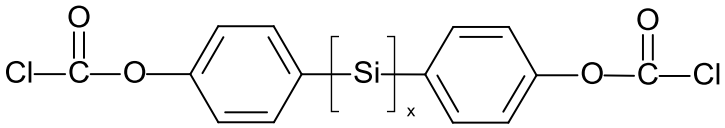
**Table 3.1** Examples of siloxane comonomers used for the synthesis of copolycarbonates [13].

Chemical Structure	Name
	4-allyl-2-methylphenol siloxane bisphenol
	4-allylphenol siloxane bisphenol
	eugenol siloxane bisphenol
	4-allyloxyphenol siloxane bisphenol

This compound is comprised of a polysiloxane chain end-capped at both ends by phenolic groups. The siloxanes shown in Table 3.1 have a siloxane block of chain lengths from 1 to about 100 [13]. Polysiloxanes are a viscous liquid at room temperature and is soluble only in the organic phase (methylene chloride) of the interfacial polymerization system. Present in the organic phase, the siloxane comonomers react with phosgene and other oligomeric and polymeric species within the organic phase. Depending on the overall content of siloxane, distribution and structure, the properties of the polymer may vary. It is the goal of this study to predict the incorporation of siloxane through a functional group model approach.

### 3.2 Copolymerization Kinetics

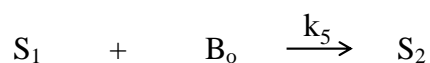
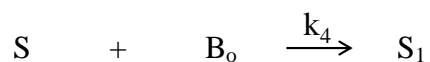
With the addition of the comonomer, the model equations that are derived above are altered to reflect this addition. A new kinetic rate constant,  $k_4$ , is introduced. This is the rate constant for reactions involving the siloxane comonomer. The chemical structure of siloxane and the two species of siloxane with modified end groups are illustrated below.

<u>Chemical Species</u>	<u>Label</u>
	<b>S</b>
	<b>S<sub>1</sub></b>
	<b>S<sub>2</sub></b>

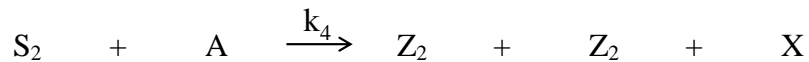
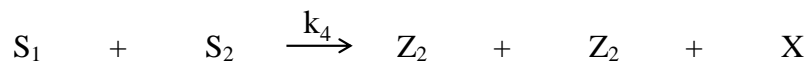
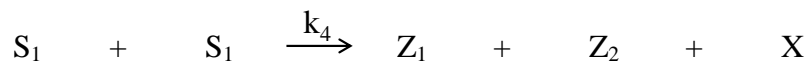
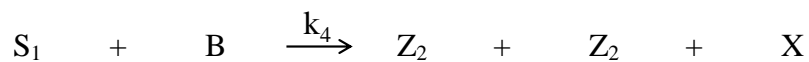
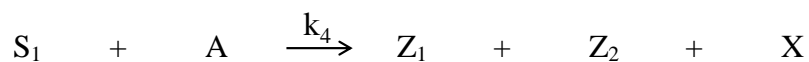
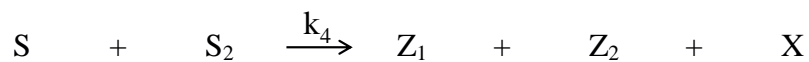
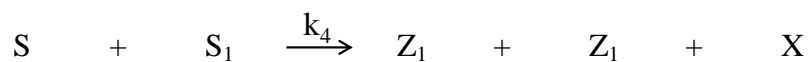
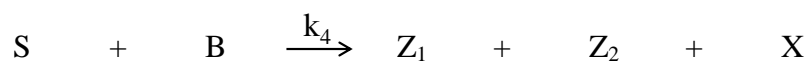
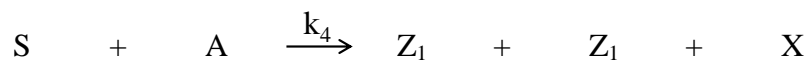
The siloxane used in this copolymerization process has a polysiloxane blocks (represented by [Si] above) of length  $x$ . Species S has two phenolic end groups. When S reacts with phosgene in the organic phase, Species S<sub>1</sub>, which has one phenolic end group and one chloroformate end group, is produced. One more reaction with phosgene produces S<sub>2</sub> which has two chloroformate end groups.

With siloxane added as a comonomer to our homopolymerization system, we must incorporate a number of additional reactions involving siloxane in our copolymerization model as outlined below. We define some new kinetic rate constants,  $k_4$  (siloxane reaction) and  $k_5$  (siloxane reaction with phosgene in the organic phase).

- **Siloxane end unit conversion** (organic phase)

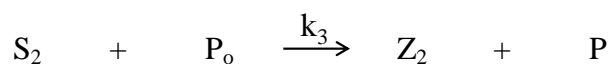
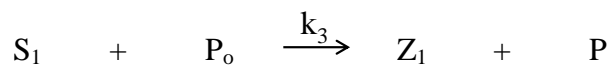
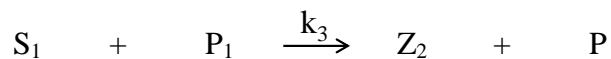
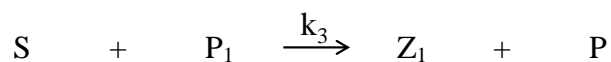


- **Siloxane monomer reactions** (organic phase)

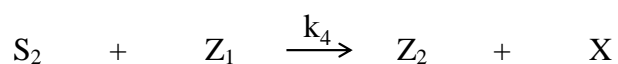
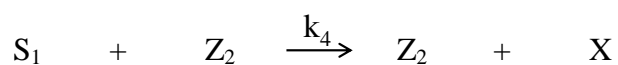
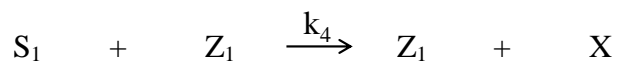
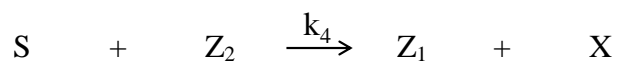




- **Siloxane reaction with chain stopper** (organic phase)



- **Siloxane reaction with polymer species** (organic phase)



As before, species X denotes the carbonate linkage between monomer units that are formed as monomers are incorporated into the polymer. Although it is not possible to calculate the number average molecular weight with the functional group model of the copolymerization system, the tracking of carbonate linkages allows us to calculate the average degree of polymerization as the copolymerization process proceeds.

In our copolymerization process simulation study, our goal is to understand how the system will behave when certain parameters are varied. The parameters pertaining to this study are siloxane feed rate, siloxane kinetic rate constant and siloxane inlet layout.

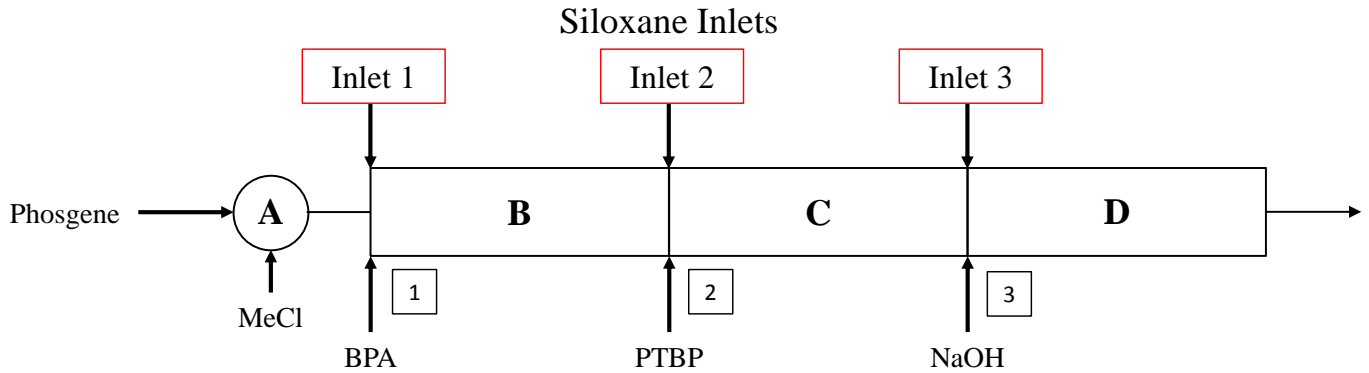


**Figure 3.1** Siloxane inlets on tubular reactor system

Figure 3.1 depicts the tubular reactor system for the copolymerization. There are 3 points available for the injection of siloxane comonomer. The siloxane concentration is given by the weight % of siloxane in the feed. Although phosgene is fed to the PFR at Zone A, BPA is fed at inlet 1 and siloxane can be fed through inlets 1, 2 or 3, the weight fraction of siloxane is calculated from the overall feed rate of all 3 monomers (phosgene, BPA, siloxane). The following equation gives the weight fraction of siloxane

$$W_{\text{siloxane}} = \frac{m_{\text{siloxane}}}{m_{\text{siloxane}} + m_{\text{phosgene}} + m_{\text{BPA}}} \quad (28)$$

where  $m_i$  is the mass flow rate of the  $i$ -component. According to GE patents on melt copolymerization and interfacial copolymerization, the siloxane content in siloxane-polycarbonate copolymers varies from 0.1 to 40 wt% of total comonomers [12,13,14]. The siloxane content of the copolymer affects the copolymer properties significantly. For example, with a large weight percent of siloxane in the copolymer, the siloxane blocks have the effect of decreasing  $T_g$ . Further, the siloxane content affects the flame retardancy and melt processability; the higher the siloxane content, the more flame retardancy and flow processability is enhanced. It is important to note that there is a threshold, past which, the copolymer becomes hazy, rendering it useless for optics or other applications where transparency is important. The mean sequence length of siloxane comonomer units and the sequence length distributions of siloxane can be estimated based on the probabilities of reactions of siloxane and BPA. We can also predict the composition and distribution of copolymers produced. It is our conclusion that, with lower weight fractions of siloxane injected early in the PFR (e.g. inlet 1), we can obtain copolymers with a random distribution of siloxane in the copolymer chain, and with higher weight fractions injected in the downstream section of the PFR (e.g. inlet 3), we can obtain longer siloxane units or siloxane-polycarbonate block copolymers. The difference between the random and block copolymers is that in block copolymers, there would be alternating aliphatic soft segments (from siloxane) and aromatic hard segments (from polycarbonate); the hard segments would agglomerate into crystalline micro domains while the soft segments remain amorphous [18].

Siloxane-PC copolymers have been found to exhibit better low temperature impact, good weatherability, improved ignition resistance, better hydrolytic stability, slowed aging, and better optical clarity. Depending on the overall siloxane content and the structure (random vs. block) of the copolymers, the copolymers may exhibit different enhancements of end-user properties.

### 3.3 Mean Sequence Length

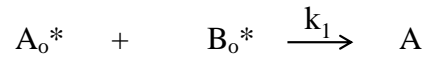
For the copolymerization process model, the overall siloxane content of polymers produced can be calculated based on the amount of siloxane that is fed to the reactor and what injection points are used. We also looked at the probabilities of reaction to determine whether or not it would be likely that multiple siloxane units be incorporated into the copolymer chain at one time. Specifically, the mean sequence length can be calculated using the following equations [19].

$$l_1 = r_1 \frac{M_1}{M_2} + 1 \quad (29)$$

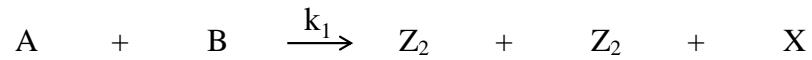
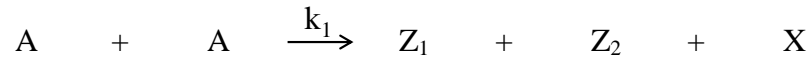
$$l_2 = r_2 \frac{M_2}{M_1} + 1 \quad (30)$$

$l_1$  is the mean sequence length of siloxane units and  $l_2$  is the mean sequence length of BPA units for a given reactivity ratio and monomer feed composition. The reactivity ratios are given by  $r_1$  and  $r_2$ , where  $r_1 = k_4 / k_1$  and  $r_2 = k_1 / k_4$  ( $k_1$  is the kinetic rate constant of BPA and  $k_4$  is the kinetic rate constant of siloxane). The rate of reactions involving BPA (listed in the following) is governed by the kinetic rate constant  $k_1$ .

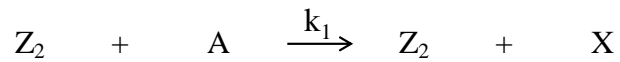
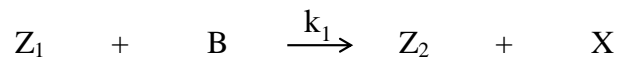
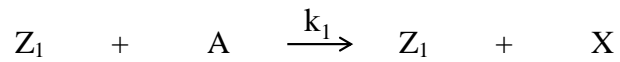
- **Phosgenation** (interface)



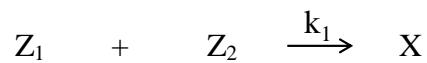
- **Reactions between monomer units** (organic phase)



- **Reactions between monomer units and polymer species** (organic phase)

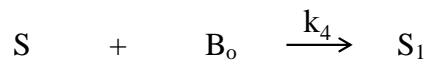


- **Reactions between polymer species** (organic phase)

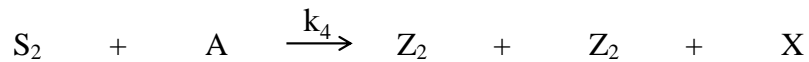
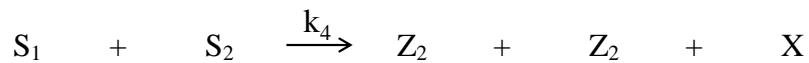
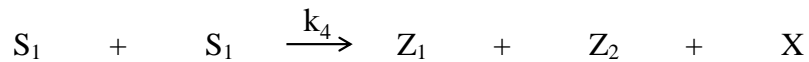
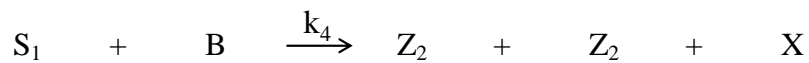
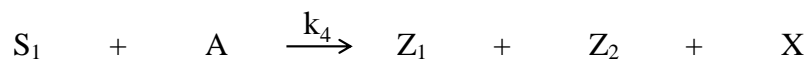
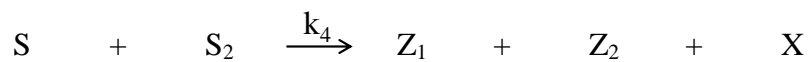
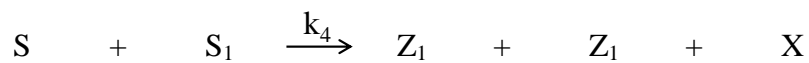
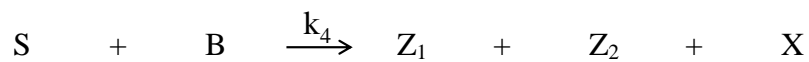
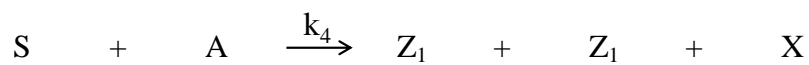


The rate of reactions involving siloxane in the organic phase follows the kinetic rate constant  $k_4$ , and these reactions are listed below for reference.

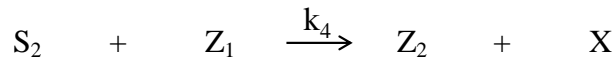
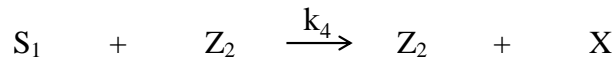
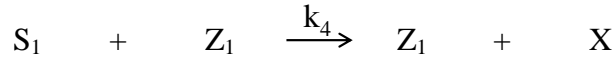
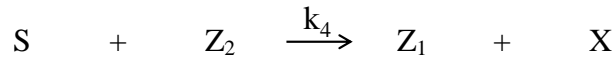
- **Siloxane end unit conversion** (organic phase)



- **Siloxane monomer reactions** (organic phase)



- **Siloxane reaction with polymer species** (organic phase)



Thus, we must consider  $k_1$  and  $k_4$  to determine the reactivity ratios for the calculation of the mean sequence lengths.

$M_1$  and  $M_2$  are the molar flow rates of siloxane and BPA, respectively. Since equations (29) and (30) do not take into account any mass transfer processes, we cannot use the molar concentrations since BPA and siloxane are dissolved in separate phases. Thus, we consider the total molar flow rate of the two components. There are three inlets available for the siloxane feed. The mean sequence lengths for 4 different configurations were determined: injection point 1, injection point 2, injection point 3, and injection points 1+2+3 (a third of the siloxane is injected into each of the three points). For each configuration, we considered 5, 10, 20, and 30 weight% (of total initial mass feed rates of BPA, phosgene and siloxane) siloxane feeds. The results are tabulated in the following sections.

### 3.3.1 Case I: Different Reactivities

For the case of different reactivities, due to the absence of kinetic rate data for allyl-phenol siloxane, we choose a reasonable, arbitrary value of  $k_4$ :  $k_4=k_1/4$  to investigate the effect of reactivity ratios on the mean sequence length of siloxane in the copolymer.

**Table 3.2** Mean sequence length of Siloxane in copolymer (Inlet 1),  $k_4=k_1/4$

Injection Point 1			
Siloxane in Feed [Weight %]	$l_1$	$l_2$	$l_1:l_2$
5	1.00	665.30	1:665
10	1.00	315.67	1:316
20	1.00	140.85	1:141
30	1.01	82.58	1:83

We can see from the results that as the weight fraction of siloxane in the feed increases, the number of BPA units in between each siloxane unit decreases (i.e. rate of siloxane incorporation increases with increasing siloxane weight fraction in feed). For example, looking at Table 3.2, if siloxane is injected only into inlet 1, at 5 wt% siloxane, there are, on average, 665 BPA units in between each incorporated siloxane monomer unit. However, according to Figure



2.13, for the interfacial PC process, the average chain length of polymers is around 50. This tells us that, interestingly, with only a 5wt% siloxane feed rate, it is very likely that not all polymer chains will have siloxane units incorporated. At 30 wt% siloxane, the average number of BPA units between each siloxane monomer unit decreases to 83.

**Table 3.3** Mean sequence length of Siloxane in copolymer (Inlet 2),  $k_4=k_1/4$

Injection Point 2			
Siloxane in Feed, [Weight %]	$l_1$	$l_2$	$l_1:l_2$
5	1.04	25.76	1:26
10	1.08	12.73	1:13
20	1.19	6.21	1:6
30	1.32	4.04	1:4

**Table 3.4** Mean sequence length of Siloxane in copolymer (Inlet 3),  $k_4=k_1/4$ 

Injection Point 3			
Siloxane in Feed, [Weight %]	$l_1$	$l_2$	$l_1:l_2$
5	1.07	15.20	1:15
10	1.15	7.73	1:8
20	1.33	3.99	1:4
30	1.57	2.74	2:3

Moreover, the further down along the PFR siloxane is fed, the shorter the length between each siloxane unit. Consider the case of a 5 wt% siloxane feed: if the first injection point is used, there are 665 BPA units separating each siloxane unit, while if the third injection point is used (Table 3.4), there are 15 BPA units separating each siloxane unit on average. When siloxane is fed to the PFR using inlet 1, siloxane is incorporated into the copolymer chain occasionally because the concentration of BPA is much higher. Alternatively, if inlet 3 is used, siloxane is added much more frequently since the concentration of BPA has decreased significantly due to the reactions upstream (the concentration of BPA at inlet 1 is  $630.17 \text{ mol/m}^3$  whereas at inlet 3,

the concentration is 13.45 mol/m<sup>3</sup> for Grade 3 PC (Table 2.4)). When inlets 2 or 3 are used for the siloxane feed, the mean sequence length given does not take into account the polymers that were already formed up to that point. Although siloxane is added to the copolymer chain more frequently, there will still be long polycarbonate domains that were produced upstream of the second and third inlets. The chain length distribution curves in Figure 2.15 can be used to determine the average length of polycarbonate domains produced upstream.

**Table 3.5** Mean sequence length of Siloxane in copolymer (Inlets 1+2+3),  $k_4=k_1/4$

Injection Point	Zone B		Zone C		Zone D		Zone B	Zone C	Zone D
1+2+3	(z=0-0.33)		(z=0.33-0.65)		(z=0.65-1.0)		B	C	D
Siloxane in Feed, [Weight %]	l <sub>1</sub>	l <sub>2</sub>	l <sub>1</sub>	l <sub>2</sub>	l <sub>1</sub>	l <sub>2</sub>	l <sub>1</sub> :l <sub>2</sub>	l <sub>1</sub> :l <sub>2</sub>	l <sub>1</sub> :l <sub>2</sub>
5	1.00	1993.9	1.01	75.25	1.02	43.52	1:1994	1:75	1:44
10	1.00	945.01	1.03	36.17	1.05	21.14	1:945	1:36	1:21
20	1.00	420.56	1.06	16.63	1.11	9.95	1:421	1:17	1:10
30	1.00	245.74	1.11	10.12	1.19	6.22	1:246	1:10	1:6

Table 3.5 shows the mean sequence lengths obtained from Zones B, C, and D when all three injections points are used for the siloxane feed. The last three column of Table 4 show the ratios of siloxane mean sequence length to BPA mean sequence length. We can conclude from these results that using all three inlets would result in copolymers that have single siloxane units spaced by varied sequence lengths of BPA. It is also apparent that, out of all the cases presented in Tables 3.2-3.5 , the only case where consecutive units of siloxane in the copolymer chain is prevalent is 30wt% siloxane fed into inlet 3.

### 3.3.2 Case II: Equal Reactivities

With equal reactivities ( $r_1 = r_2 = 1$ ), the following results are obtained for the mean sequence length of siloxane.

**Table 3.6** Mean sequence length of Siloxane in copolymer (Inlet 1),  $k_4=k_1$

Injection Point 1			
Siloxane in Feed, [Weight %]	$l_1$	$l_2$	$l_1:l_2$
5	1.00	167.08	1:167
10	1.01	79.67	1:80
20	1.03	35.96	1:36
30	1.05	21.40	1:21

**Table 3.7** Mean sequence length of Siloxane in copolymer (Inlet 2),  $k_4=k_1$ 

Injection Point 2			
Siloxane in Feed, [Weight %]	$l_1$	$l_2$	$l_1:l_2$
5	1.16	7.19	1:7
10	1.34	3.93	1:4
20	1.77	2.30	2:2
30	2.32	1.76	2:2

**Table 3.8** Mean sequence length of Siloxane in copolymer (Inlet 3),  $k_4=k_1$ 

Injection Point 3			
Siloxane in Feed, [Weight %]	$l_1$	$l_2$	$l_1:l_2$
5	1.28	4.56	1:5
10	1.59	2.68	2:3
20	2.34	1.75	2:2
30	3.29	1.44	3:1

**Table 3.9** Mean sequence length of Siloxane in copolymer (Inlets 1+2+3),  $k_4=k_1$ 

Injection Point	Zone B		Zone C		Zone D		B	C	D
	(z=0-0.33)		(z=0.33-0.65)		(z=0.65-1.0)				
1+2+3									
Siloxane in Feed, [Weight %]	$l_1$	$l_2$	$l_1$	$l_2$	$l_1$	$l_2$	$l_1:l_2$	$l_1:l_2$	$l_1:l_2$
5	1.00	499.23	1.05	19.58	1.09	11.67	1:499	1:20	1:12
10	1.00	237.00	1.11	9.80	1.20	6.05	1:237	1:10	1:6
20	1.01	105.89	1.26	4.91	1.45	3.25	1:106	1:5	1:3
30	1.02	62.19	1.44	3.28	1.76	2.31	1:62	1:3	2:2

Compared to the previous case of different reactivities ( $k_4=k_1/4$ ), with equal reactivity of BPA and Siloxane, the mean sequence lengths of BPA units are all shorter regardless of siloxane feed composition or siloxane inlet configuration due to the relatively higher reactivity of siloxane. Further, we see that consecutive siloxane units are more likely with a siloxane feed composition of only 20 weight percent at inlet 2, whereas before, with a lower reactivity for siloxane, consecutive siloxane units were not probable until a 30 weight percent siloxane feed at inlet 3.

### 3.4 Sequence Length Distribution

Another way of investigating the composition distribution of the siloxane-copoly carbonate copolymers is to look at the sequence length distribution. The sequence length distribution gives us the probabilities of  $x$ -unit sequences for both siloxane units and PC units. The sequence length distributions for siloxane (denoted by the subscript 1) and for BPA (denoted by the subscript 2) can be calculated using the following equations [20],

$$(N_1)_x = (P_{11})^{x-1}P_{12} \quad (31)$$

$$(N_2)_x = (P_{22})^{x-1}P_{21} \quad (32)$$

where  $P_{11} = \frac{r_1[S]}{r_1[S]+[BPA]}$ ,  $P_{12} = \frac{[BPA]}{r_1[S]+[BPA]}$ ,  $P_{21} = \frac{[S]}{r_2[BPA]+[S]}$ ,  $P_{22} = \frac{r_2[BPA]}{r_2[BPA]+[S]}$

$P_{11}, P_{12}$  denote the probabilities of reactions involving siloxane units and  $P_{22}, P_{21}$  denote the probabilities of reactions that involve BPA units. Given that  $x$  (a positive integer) is the sequence length,  $(N_1)_x$  is the probability of a sequence of  $x$  siloxane unit(s). Using these equations, the sequence length distributions for a variety of cases, with different siloxane feed compositions and different siloxane inlet configurations, can be determined. The results are discussed in sections 3.4.1, 3.4.2 and 3.4.3.

### 3.4.1 Case I: Siloxane Injection in Point 1

Here, we only include data from the case of different reactivities, namely  $k_4=k_1/4$ , for brevity as the case of equal reactivities exhibits an almost identical pattern with the only difference being that the case of equal reactivities shows generally higher values for the siloxane sequence length distribution.

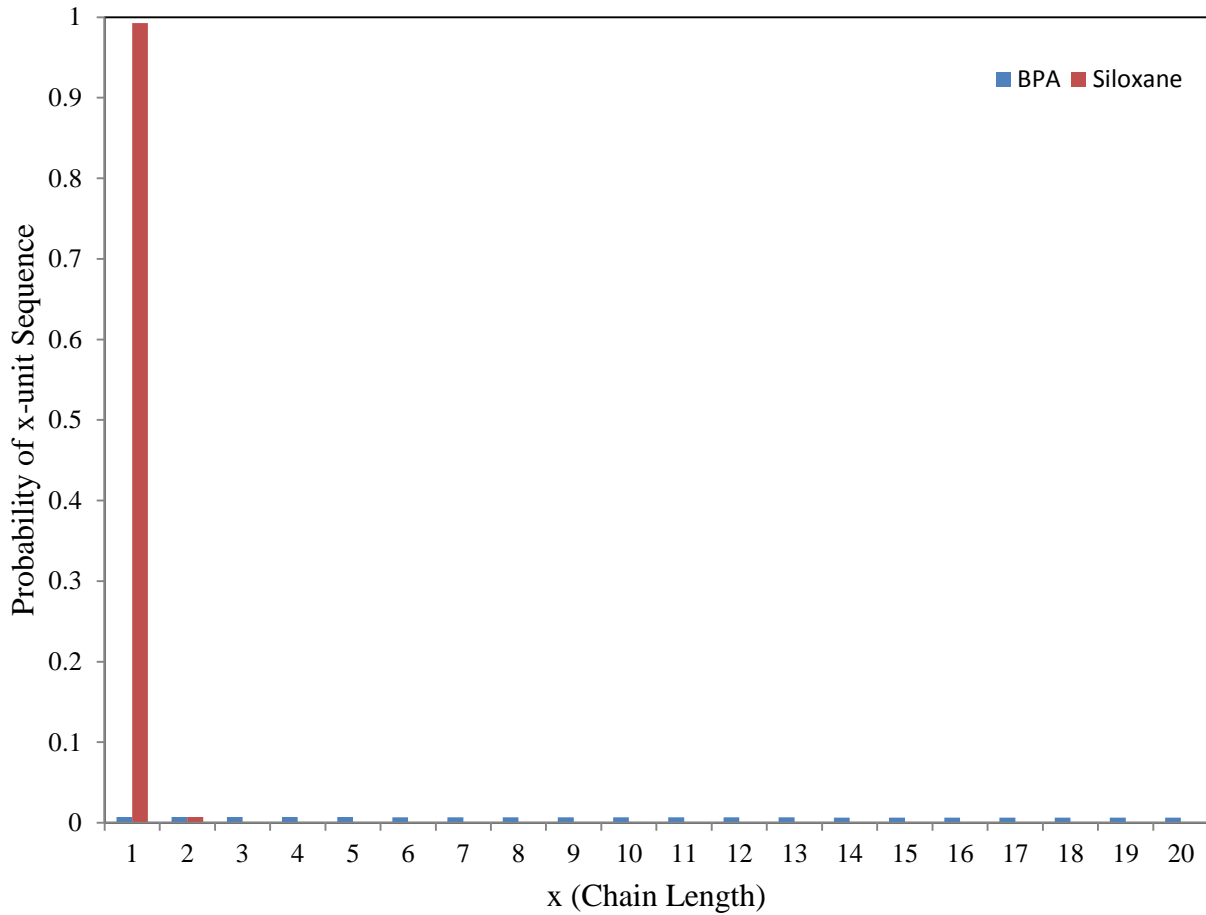


**Figure 3.2** Siloxane sequence length distribution (Siloxane inlet 1,  $k_4=k_1/4$ , 10wt% Siloxane Feed)



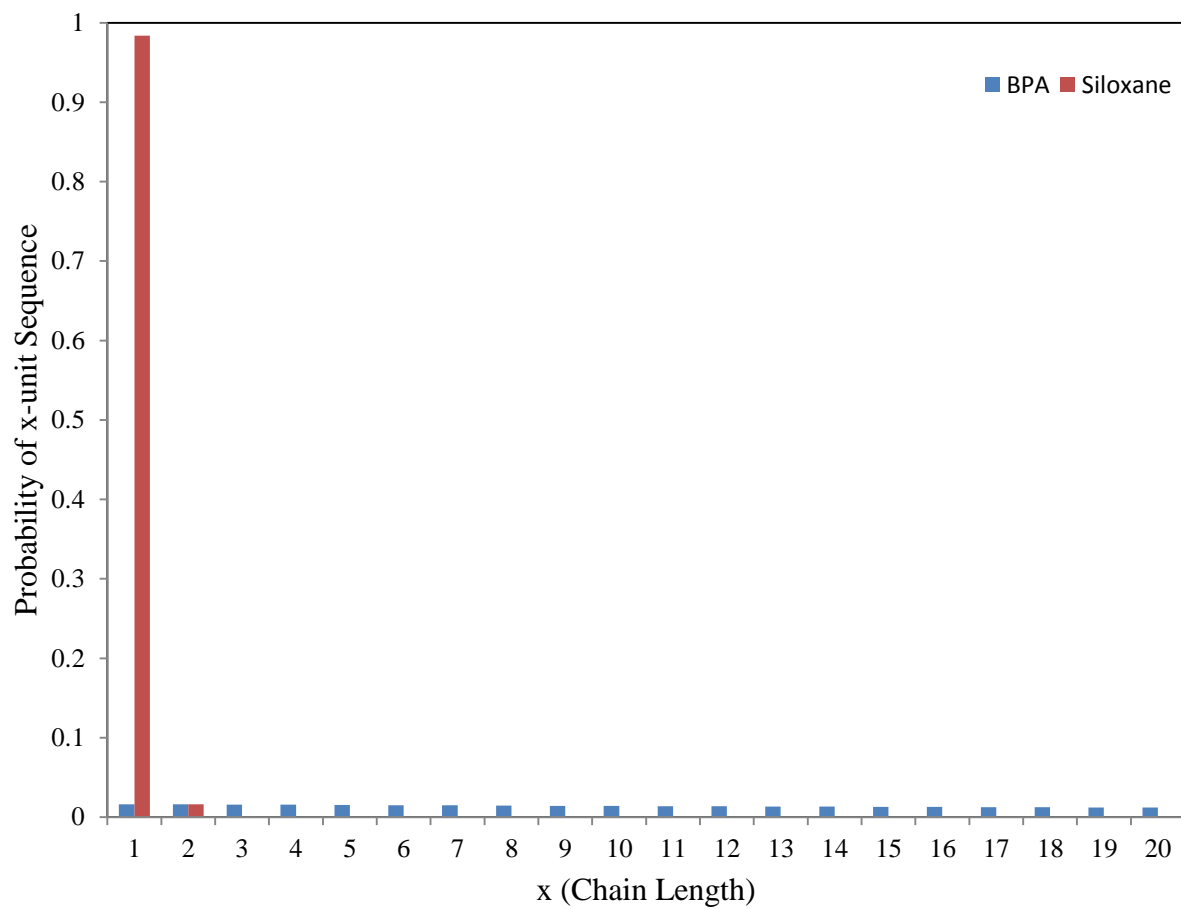


**Figure 3.3** Siloxane sequence length distribution (Siloxane inlet 1,  $k_4=k_1/4$ , 20wt% Siloxane Feed)

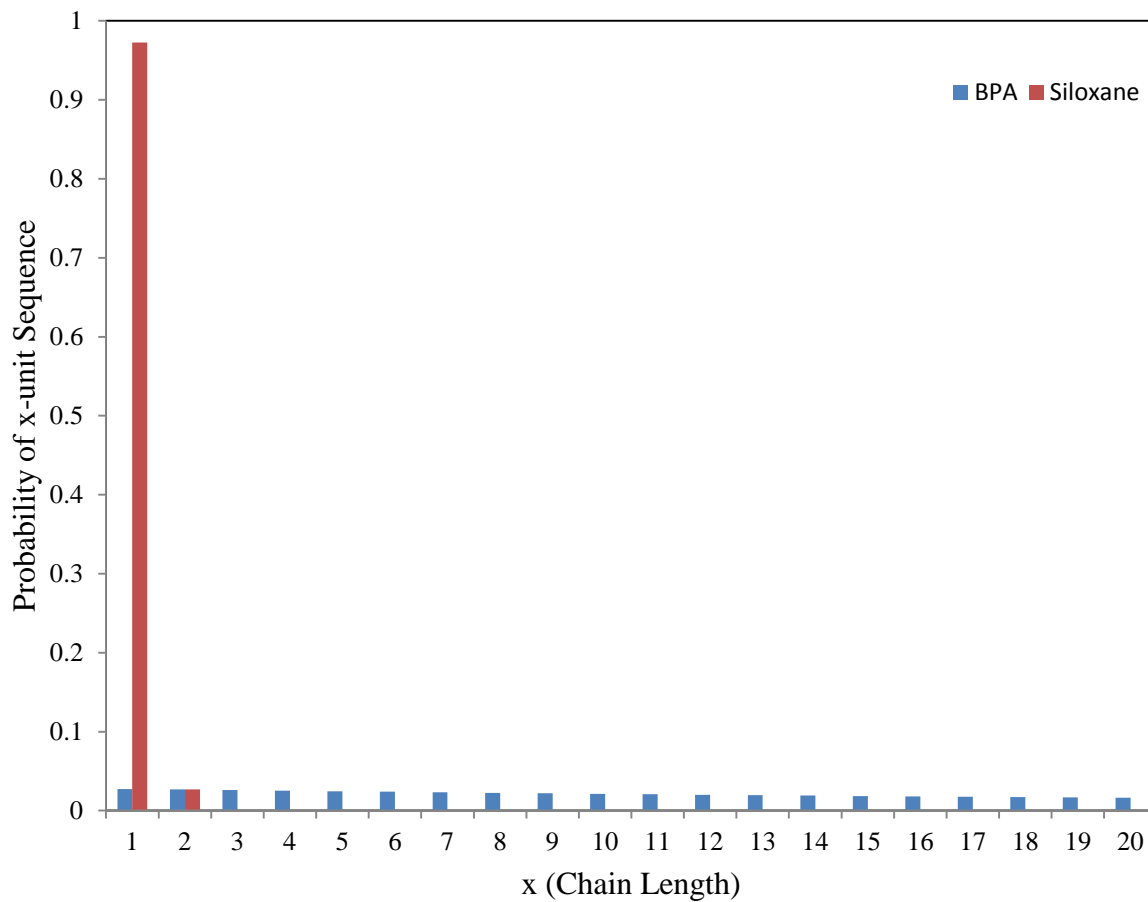


**Figure 3.4** Siloxane sequence length distribution (Siloxane inlet 1,  $k_4=k_1/4$ , 30wt% Siloxane Feed)

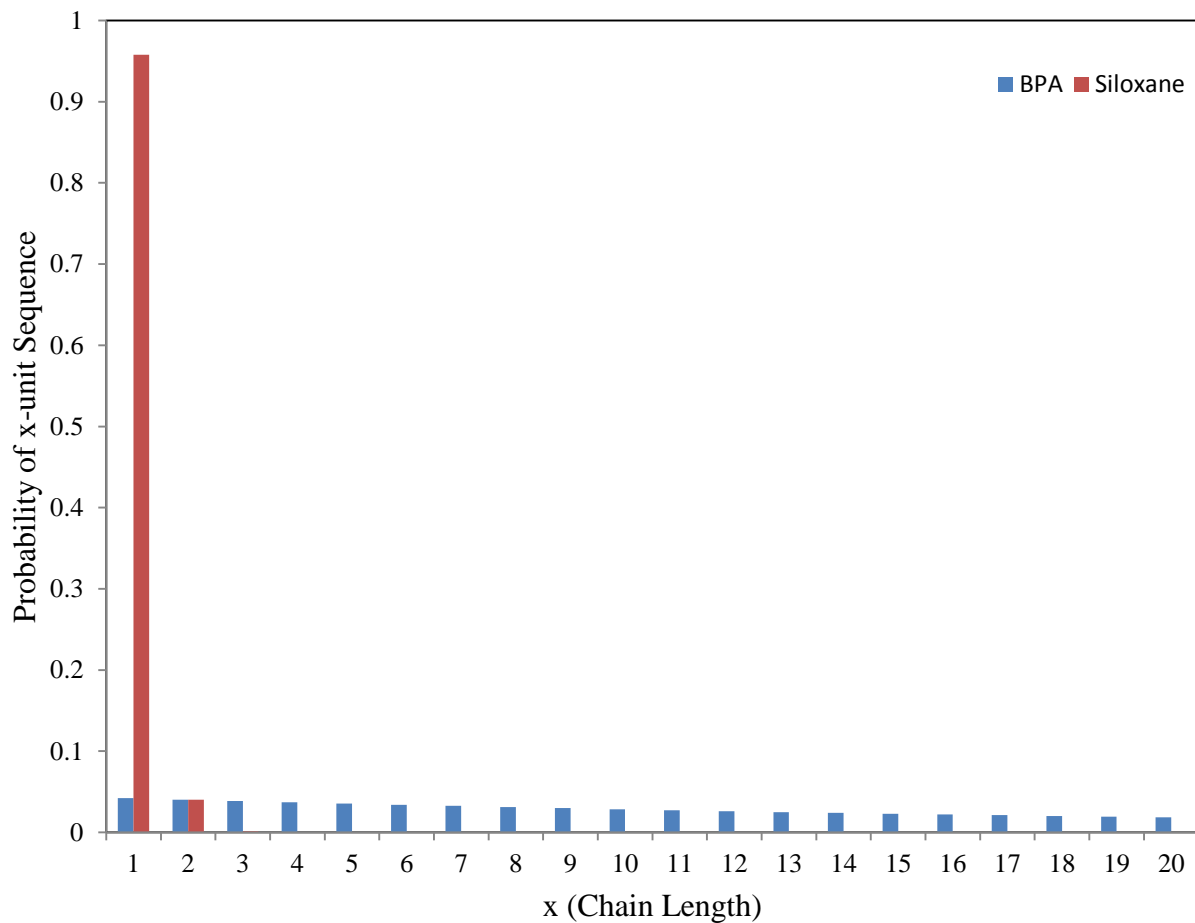


**Figure 3.5** Siloxane sequence length distribution (Siloxane inlet 1,  $k_4=k_1/4$ , 40wt% Siloxane Feed)

Figures 3.2-3.5 give the sequence length distributions for the case of using only siloxane inlet 1. We can see that when using siloxane inlet 1, whether the siloxane feed composition is 10, 20, 30, or 40 weight percent, over 95% of the siloxane units incorporated into the copolymer chain will have a sequence length of 1. With 10, 20, and 30 weight percent of siloxane, Figures 3.2-3.4 show that, although miniscule, there is a possibility of a siloxane sequence length of 2 units and a siloxane sequence of 3 units. With 40wt% siloxane (Figure 3.5), we see a small probability of a 4-unit siloxane sequence. However, overall, we would most likely have a vast majority of 1-unit sequences of siloxane incorporated into the copolymer chain when inlet 1 is used, and this is a reasonable result knowing that the siloxane polymer chains are much larger and bulkier than the PC monomer units.

### 3.4.2 Case II: Siloxane Injection in Point 2

The following results are obtained for the sequence length distribution if inlet 2 is used.

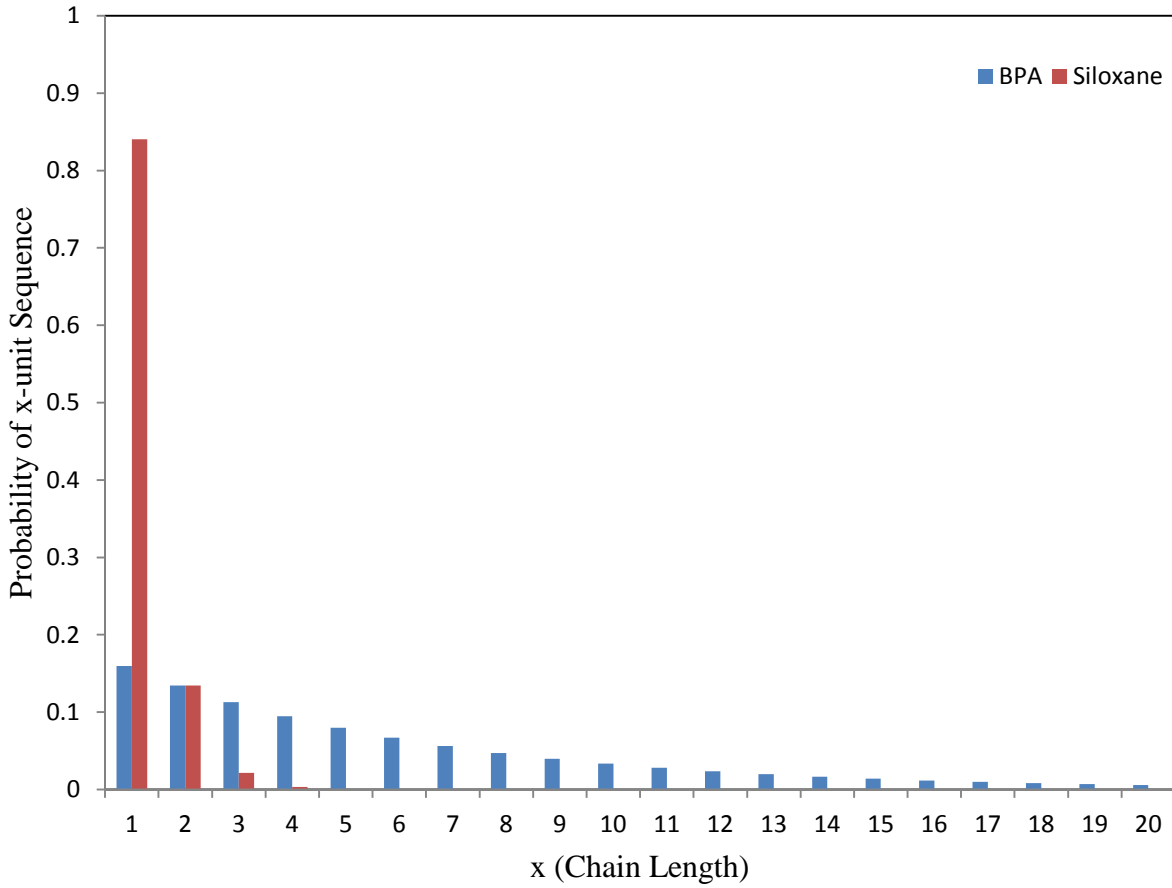


**Figure 3.6** Siloxane sequence length distribution (Siloxane inlet 2,  $k_4=k_1/4$ , 10wt% Siloxane Feed)

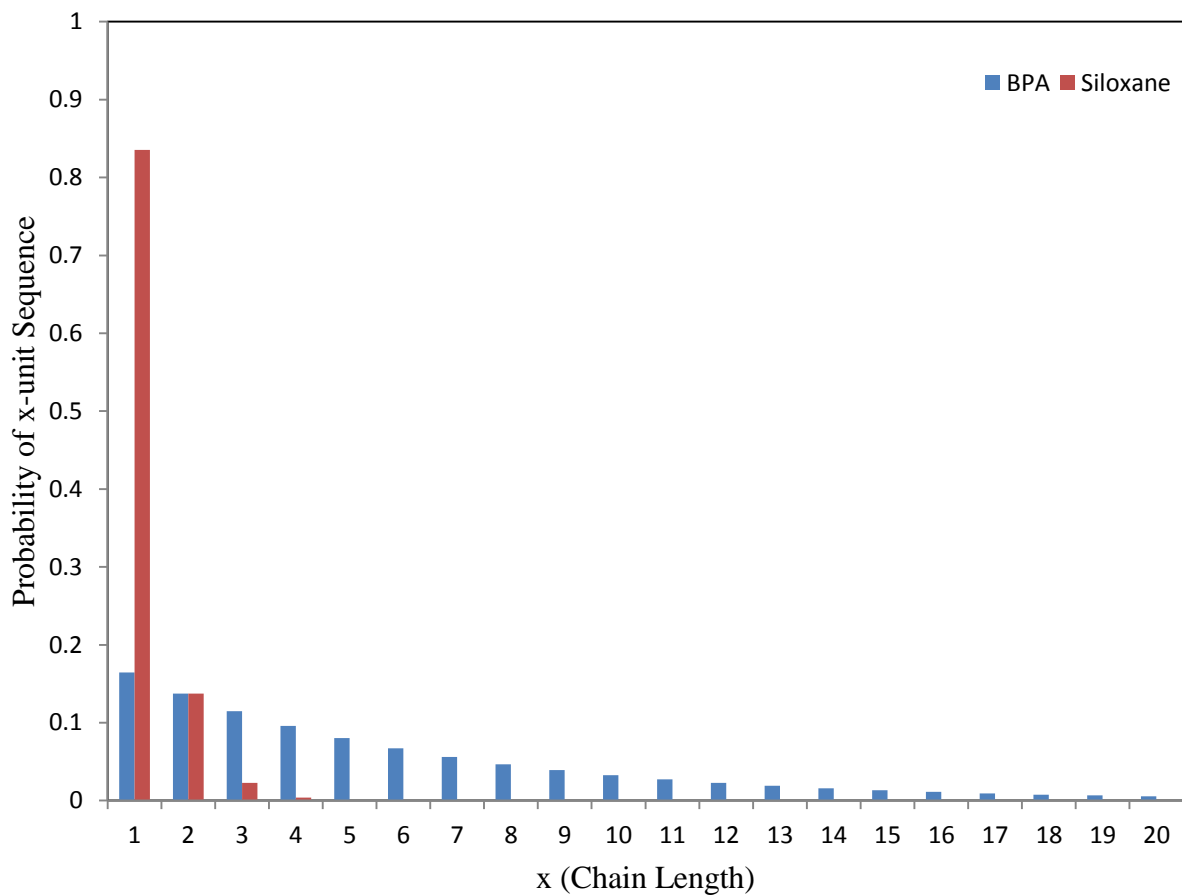


**Figure 3.7** Siloxane sequence length distribution (Siloxane inlet 2,  $k_4=k_1/4$ , 20wt% Siloxane Feed)

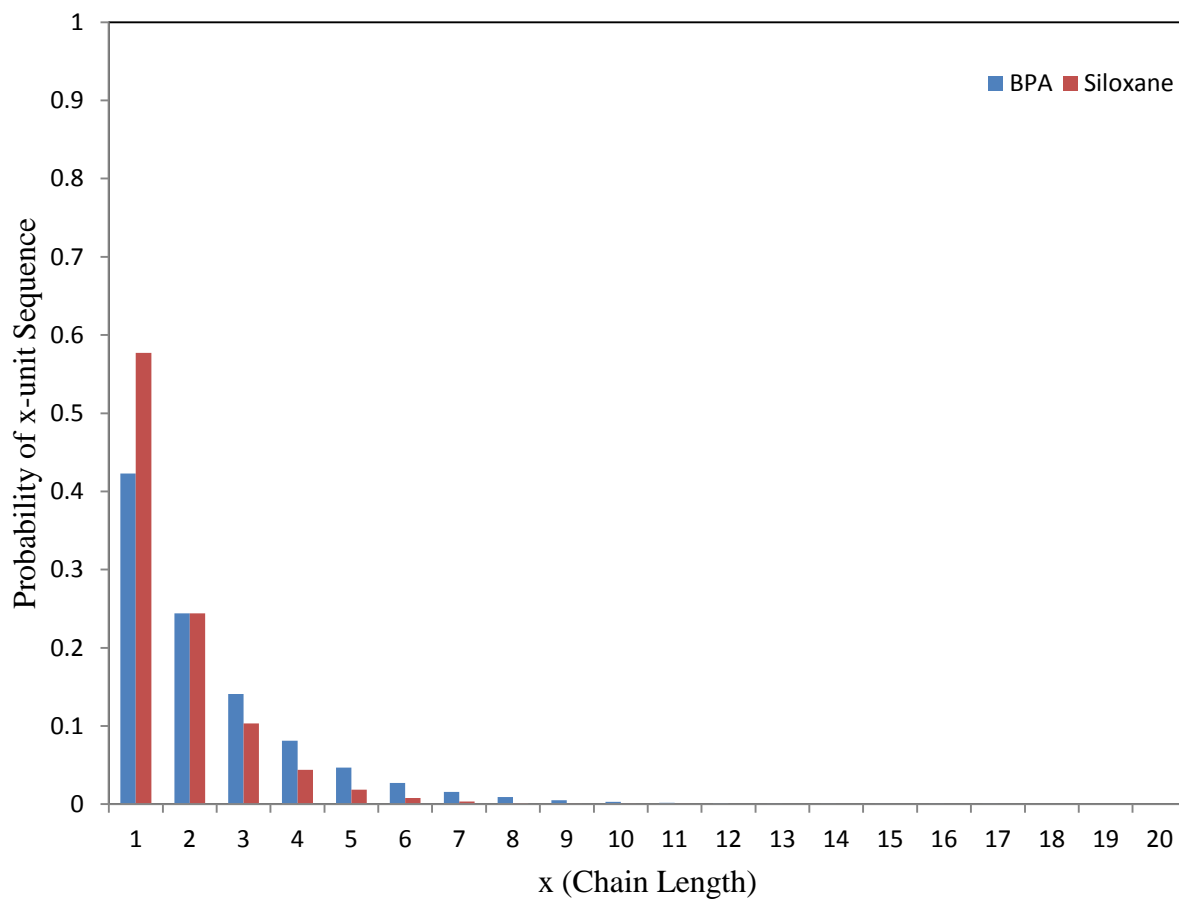


**Figure 3.8** Siloxane sequence length distribution (Siloxane inlet 2,  $k_4=k_1/4$ , 30wt% Siloxane Feed)

Using siloxane inlet 2, probabilities for siloxane sequence lengths of greater than 1 increase compared to the previous case. When siloxane is added to the reactor at inlet 2, the probability of reaction for siloxane increases because the concentration of BPA has decreased during the reactions that occur in Zone B of the PFR (between inlets 1 and 2). For this reason, even if the siloxane feed composition is the same, using inlet 2 will present a higher probability of siloxane sequences of more than 1 unit compared to the previous case of using siloxane inlet 1. However, it is important to note that the sequence length distributions presented here are calculated from the concentrations of the two co-monomers at inlet 2. Thus, the cases of inlet 2 and inlet 3 do not take into account the polycarbonate chains that have been polymerized upstream of that particular inlet. For these cases, it is important to consider the average chain length of polycarbonate chains produced upstream for a complete picture of the composition distribution.



### 3.4.3 Case 3: Siloxane injection in Point 3

Finally, the following results were obtained for the sequence length distribution in the case of inlet 3.

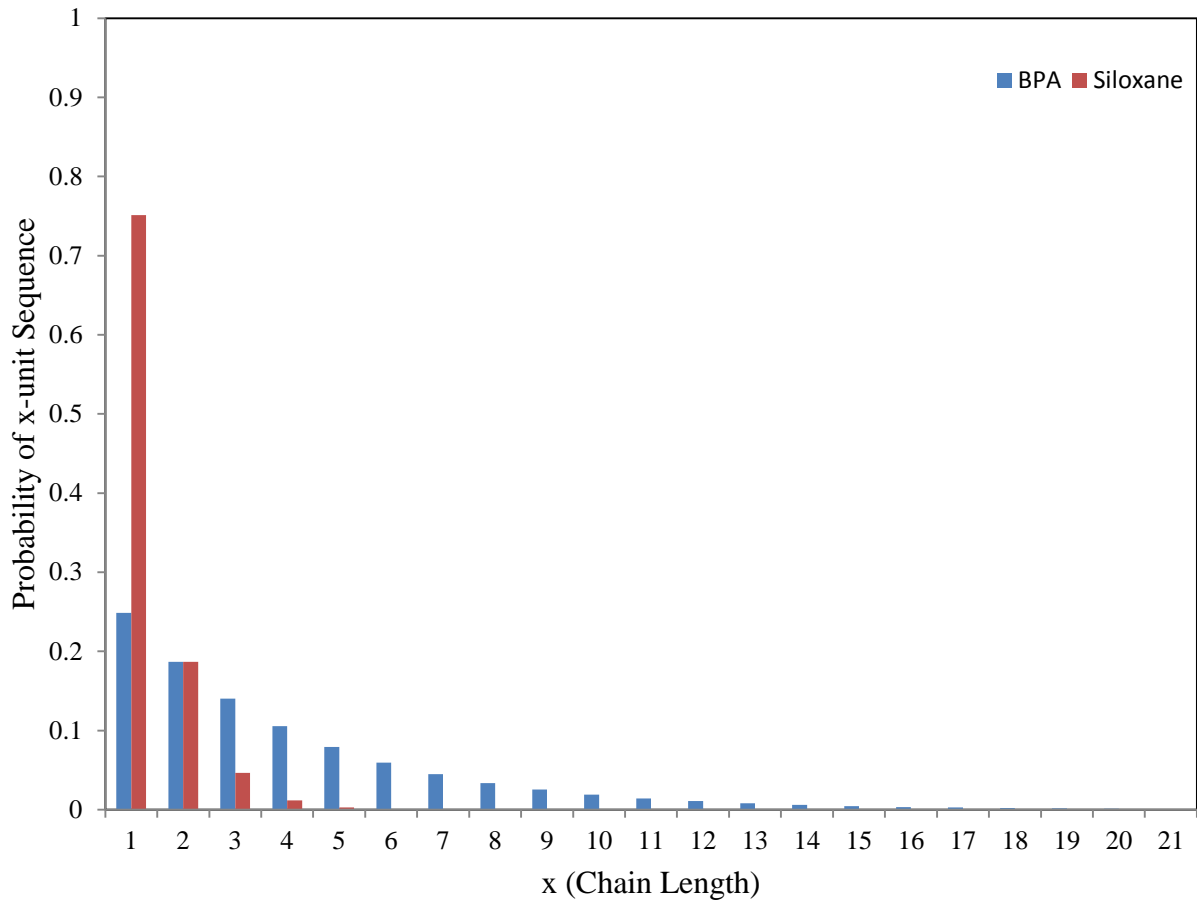


**Figure 3.9** Siloxane sequence length distribution (Siloxane inlet 3,  $k_4=k_1/4$ , 10wt% Siloxane Feed)

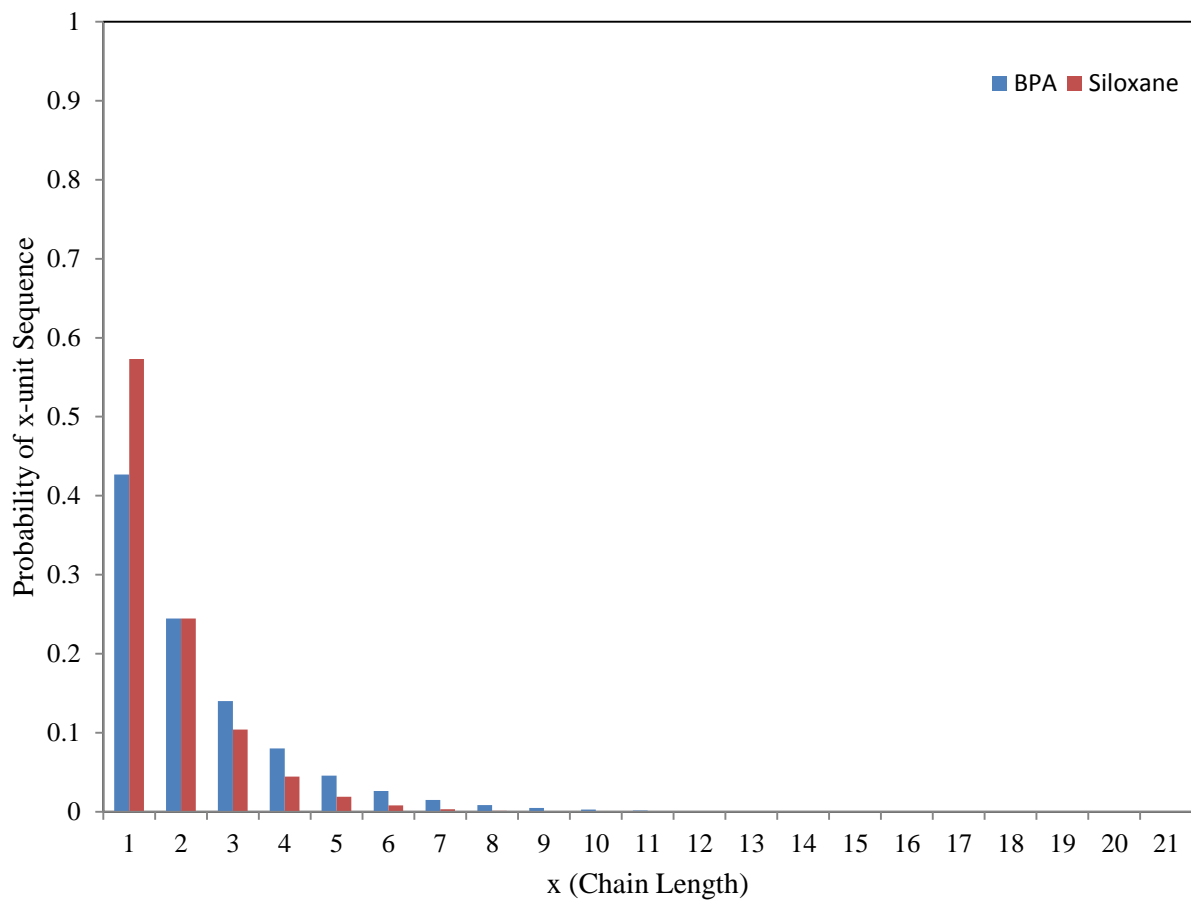


**Figure 3.10** Siloxane sequence length distribution (Siloxane inlet 3,  $k_4=k_1/4$ , 20wt% Siloxane Feed)

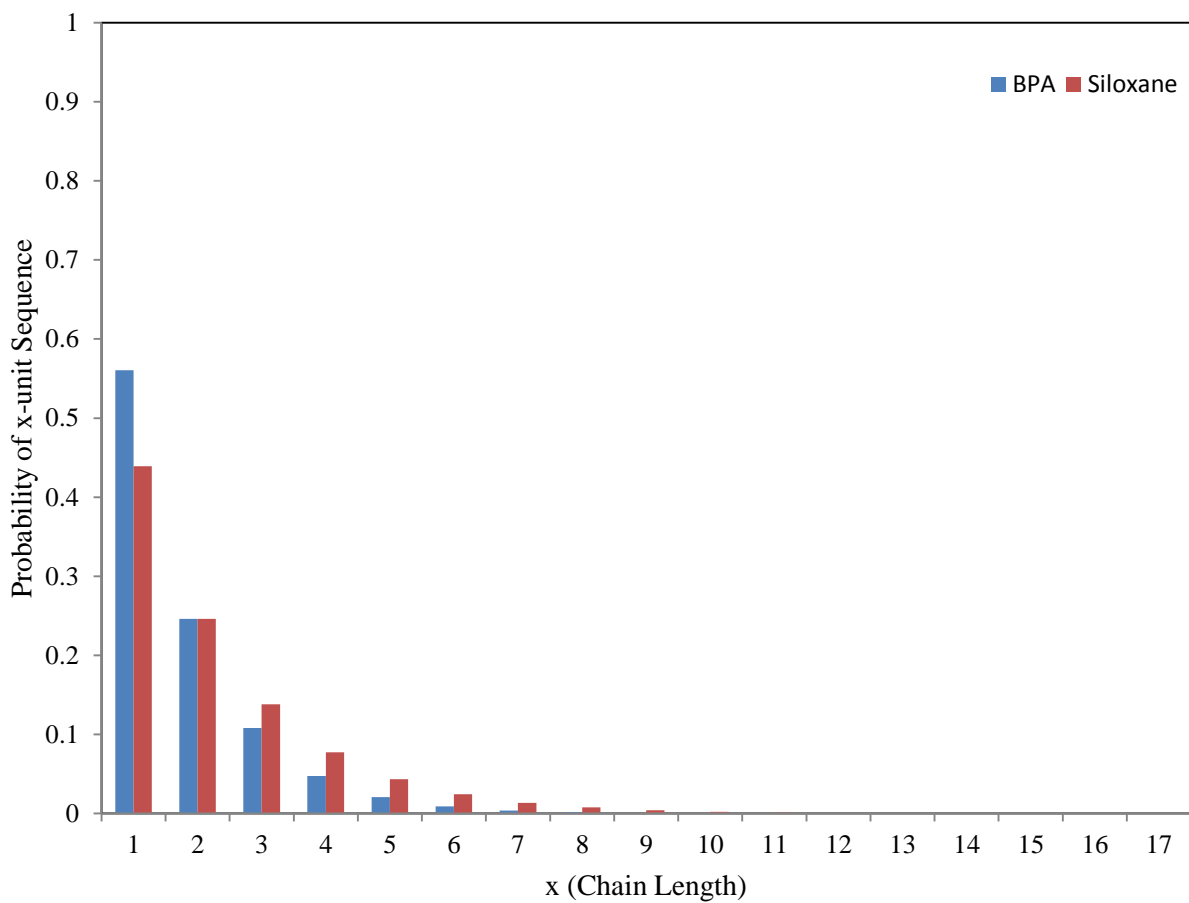


**Figure 3.11** Siloxane sequence length distribution (Siloxane inlet 3,  $k_4=k_1/4$ , 10wt% Siloxane Feed)

The trend observed in comparing the cases of inlet 1 and inlet 2 is the same trend we see when comparing the cases of inlet 2 and using inlet 3. The probability of reaction for siloxane is even higher when inlet 3 is used because the concentration of BPA has decreased further from inlet 2 to inlet 3. Looking at the sequence length distributions, the case of inlet 3 would be the ideal condition for trying to produce siloxane-polycarbonate block copolymers due to the high likelihood for siloxane sequence of more than 1 unit. Conversely, using inlet 1 would be ideal for creating random siloxane-polycarbonate copolymers.

### **3.5 Conclusion**

The functional group model of the interfacial process has been augmented with the inclusion of an additional comonomer, allyl-phenol siloxane. We defined the chemical reactions involving siloxane and the different configurations for the siloxane feed. We presented a case study for this copolymerization system by investigating the effects of the siloxane feed composition and siloxane inlet configuration on the copolymer composition, more specifically the mean sequence length and sequence length distribution of siloxane and BPA segments. Specifically, we have seen that the monomer reactivities, feed compositions and inlet configurations have a significant impact on the copolymer composition. As expected, the cases with relatively higher probabilities of reactions involving siloxane (e.g. equal reactivity of siloxane and BPA, higher siloxane composition in feed, and injection of siloxane into inlets further down the tubular reactor) predict higher probabilities of siloxane segments of more than one unit. Conversely, cases with relatively lower probabilities of siloxane reactions show longer BPA segments and shorter siloxane segments.

## Chapter 4. Summary

In this study, the kinetics of the interfacial process in a tubular reactor was investigated. Carefully considering, a mathematical simulation model was developed. This functional group model was then fine-tuned by optimizing the kinetic parameters (kinetic rate constants and mass transfer coefficients) using proprietary plant data. The result was a model that predicted the behavior of this system with remarkable accuracy. This functional group model was expanded to a copolymerization process model with the addition of a polysiloxane comonomer. The copolymerization model was used to examine the parameters that affect the composition of siloxane-polycarbonate copolymers.

For the interfacial polymerization system, it is evident that the mass transfer at the interface is a crucial process. The linear velocity has a significant impact on the efficacy of mixing due to the utilization of static mixers in the tubular reactor. With higher linear velocities, the average size of the dispersed aqueous droplets is smaller, which means that the surface area available for mass transfer is greater. These parameters affect the mass transfer of both BPA and phosgene from their bulk phases to the interface. However, it has been determined that the mass transfer resistance of phosgene is insignificant, thus, the mass transfer of BPA is more important in determining the properties of the polymer. We have seen that the mass transfer coefficient of BPA is an important parameter as well, as it determines whether the processes at the interface are reaction controlled or diffusion controlled. For the case of small values of the BPA mass transfer coefficient, the process is diffusion controlled, and for larger values of the mass transfer

coefficient, the process is reaction controlled. By developing this interfacial process model, we have been able to study the important dynamics of this heterophase system.

With polysiloxane as an additional comonomer in the interfacial process, siloxane-polycarbonate copolymers can be produced. These copolymers exhibit enhanced flame retardancy, processability, weathering properties and impact strength. Expanding our interfacial process model to a copolymerization model, various case studies were performed to identify the crucial parameters that affect the monomer composition and distribution of these copolymers. More specifically, we studied the mean sequence length and sequence length distribution of siloxane and BPA segments. We have determined that the monomer feed composition, the monomer reactivities, and monomer feed configuration (in the tubular reactor system) have a significant impact on the copolymer properties. Of the case studies performed, cases with a relatively high probability of reaction of siloxane, such as when siloxane is injected further down the PFR (BPA concentrations are lower), when siloxane reactivity is higher, or when the siloxane feed rate is higher, siloxane segments of chain length greater than one are more probable.

## Bibliography

1. Schnell, Hermann. "Chemistry and Physics of Polycarbonate", Interscience Publishers, New York (1964).
2. Bendler, John T. "Handbook of Polycarbonate Science and Technology", CRC Press (1999).
3. Lyu, Min-Young, Jae Sik Lee, and Youlee Pae. "Study of mechanical and rheological behaviors of linear and branched polycarbonates blends." *Journal of applied polymer science* 80.10 (2001): 1814-1824.
4. Marks, M. J., and J. K. Sekinger. "Synthesis, Crosslinking, and Properties of Benzocyclobutene-Terminated Bisphenol A Polycarbonates." *Macromolecules* 27.15 (1994): 4106-4113.
5. Kim, Yangsoo, Kyu Yong Choi, and Thomas A. Chamberlin. "Kinetics of melt transesterification of diphenyl carbonate and bisphenol A to polycarbonate with lithium hydroxide monohydrate catalyst." *Industrial & engineering chemistry research* 31.9 (1992): 2118-2127.
6. Mills, Patrick L. "Analysis of multiphase polycarbonate polymerization in a semibatch reactor." *Chemical engineering science* 41.11 (1986): 2939-2952.
7. Gu, Jen-Tau, and Chun-Shan Wang. "The interfacial polycarbonate reactions. I. Defining the critical process parameters." *Journal of applied polymer science* 44.5 (1992): 849-857.
8. Joseph Schork, F., and Wilfred Smulders. "On the molecular weight distribution polydispersity of continuous living-radical polymerization." *Journal of applied polymer science* 92.1 (2004): 539-542.

9. Theron, Félicie, Nathalie Le Sauze, and Alain Ricard. "Turbulent Liquid– Liquid Dispersion in Sulzer SMX Mixer." *Industrial & Engineering Chemistry Research* 49.2 (2009): 623-632.
10. Yaws, Carl L. "Transport Properties of Chemical and Hydrocarbons", William Andrew (2009).
11. Flory, Paul J. "Molecular Size Distribution in Linear Condensation Polymers1." *Journal of the American Chemical Society* 58.10 (1936): 1877-1885.
12. Banach, Timothy Edward, et al. "Method for making siloxane copolycarbonates." U.S. Patent No. 6,252,013. 26 Jun. 2001.
13. Phelps, Peter D., et al. "Silicone-polycarbonate block copolymers and polycarbonate blends having reduced haze, and method for making." U.S. Patent No. 5,530,083. 25 Jun. 1996.
14. Cella, James Anthony, James Ross Fishburn, and James Alan Mahood. "Polycarbonate-siloxane copolymers." U.S. Patent No. 6,630,525. 7 Oct. 2003.
15. Hoover, James F., and Paul D. Sybert. "Compositions of siloxane polycarbonate block copolymers and high heat polycarbonates." U.S. Patent No. 5,455,310. 3 Oct. 1995.
16. Hoover, James Franklin. "Polycarbonate-polysiloxane block copolymers." U.S. Patent No. 6,072,011. 6 Jun. 2000.
17. Vaughn, Howard A. "Organopolysiloxane polycarbonate block copolymers." U.S. Patent No. 3,419,634. 1968.
18. Seo, D. W., et al. "Synthesis and Properties of Polycarbonate-co-Poly (siloxane-urethane-siloxane) Block Copolymers." *Macromolecular Research* 20.8 (2012): 852-857.



19. Pazhanisamy, P., Mohamed Ariff, and Q. Anwaruddin. "Copolymers of  $\alpha$ -methylstyrene with N-cyclohexylacrylamide: Synthesis, monomer reactivity ratios, and mean sequence length." *Journal of Macromolecular Science, Part A: Pure and Applied Chemistry* 34.6 (1997): 1045-1054.
20. Liu, Xiaoxuan, et al. "Reactivity ratios and sequence structures of the copolymers prepared using photo-induced copolymerization of MMA with MTMP." *Magnetic Resonance in Chemistry* (2012).